Published online 9 August 2004

Nucleic Acids Research, 2004, Vol. 32, No. 14 4217–4223
doi:10.1093/nar/gkh753

Importance in catalysis of a magnesium ion with very low affinity for a hammerhead ribozyme

Atsushi Inoue[1,3], Yasuomi Takagi[1,2] and Kazunari Taira[1,2,3,*]

[1]Gene Function Research Center and [2]iGENE Therapeutics, Inc., National Institute of Advanced Industrial Science and Technology (AIST), Central 4, 1-1-1 Higashi, Tsukuba Science City 305-8562, Japan and [3]Department of Chemistry and Biotechnology, School of Engineering, The University of Tokyo, Hongo, Tokyo 113-8656, Japan

Received December 16, 2003; Revised and Accepted July 21, 2004

ABSTRACT

Available evidence suggests that Mg^{2+} ions are involved in reactions catalyzed by hammerhead ribozymes. However, the activity in the presence of exclusively monovalent ions led us to question whether divalent metal ions really function as catalysts when they are present. We investigated ribozyme activity in the presence of high levels of Mg^{2+} ions and the effects of Li^+ ions in promoting ribozyme activity. We found that catalytic activity increased linearly with increasing concentrations of Mg^{2+} ions and did not reach a plateau value even at 1 M Mg^{2+} ions. Furthermore, this dependence on Mg^{2+} ions was observed in the presence of a high concentration of Li^+ ions. These results indicate that the Mg^{2+} ion is a very effective cofactor but that the affinity of the ribozyme for a specific Mg^{2+} ion is very low. Moreover, cleavage by the ribozyme in the presence of both Li^+ and Mg^{2+} ions was more effective than expected, suggesting the existence of a new reaction pathway—a cooperative pathway—in the presence of these multiple ions, and the possibility that a Mg^{2+} ion with weak affinity for the ribozyme is likely to function in structural support and/or act as a catalyst.

INTRODUCTION

Naturally existing catalytic RNAs include hammerhead, hairpin, hepatitis delta virus (HDV) and Varkud Satellite (VS) ribozymes, group I and II introns, and the RNA subunit of RNase P (1–7). In addition, recent structural and chemical analyses strongly suggest that ribosomal RNA might also be a ribozyme (8–11). In addition, the possibility exists that the RNA component of the spliceosome might be a ribozyme too (12). The earliest research on ribozymes suggested that all ribozymes might be metalloenzymes that require divalent metal ions, in particular Mg^{2+} ions, for catalysis, and that all might operate by a basically similar mechanism. However, subsequent, extensive studies revealed that the catalytic activity of hairpin ribozymes is independent of divalent metal ions (7,13–18). Thus, the various types of ribozymes appear to exploit different cleavage mechanisms, which depend upon the architecture of the individual ribozyme. Even hammerhead ribozymes, which have generally been characterized as typical metalloenzymes, can no longer be categorized unambiguously.

Naturally existing hammerhead ribozymes were originally identified in some RNA viruses, and it was demonstrated that they act *in cis* during viral replication by the rolling circle mechanism (3). In the laboratory, ribozymes have been engineered such that they act *in trans* against other RNA molecules and catalyze the cleavage of phosphodiester bonds at specific sites to generate specific products, each of which has a 2′,3′-cyclic phosphate and a 5′-hydroxyl group (19–22). The transesterification mechanism includes deprotonation of the 2′-hydroxyl moiety of a ribose group, nucleophilic attack of the 2′-oxygen on the adjacent phosphorus atom, and protonation of the 5′-oxyanion leaving group (Figure 1A). A large body of evidence also indicates that the P9/$G_{10.1}$ site binds a metal ion with high affinity, with other metal ion-binding sites being located around the G_5 nucleobase and A_{13} phosphate near the site of cleavage (23–36). Thus, the idea that ribozymes are metalloenzymes has been generally accepted. However, it was reported recently that hammerhead ribozymes are active in the presence of very high concentrations of monovalent cations, such as Li^+ or NH_4^+ ions, in the absence of divalent metal ions (37). This finding raises the possibility that hammerhead ribozymes should not be classified as metalloenzymes. Therefore, we decided to investigate ribozyme activity in the presence of Mg^{2+} ions and the effects of Mg^{2+} ions in the presence of Li^+ ions on ribozyme activity, using a well-studied model hammerhead ribozyme (R32) and its substrate (S11), both of which are shown in Figure 1B (5–7,25,28,32–34,38–41).

We investigated the dependence on the concentration of Mg^{2+} and Li^+ ions of ribozyme activity over a range from 5 mM to ~1 M Mg^{2+} ions and 1 to 5 M Li^+ ions, respectively. Although several research groups have reported similar analyses (42–50), the concentrations of Mg^{2+} ions used in most of these studies were <100 mM, and little information is available about activity at a higher concentration, such as 1 M. The activity at high concentrations of Mg^{2+} ions, as compared

*To whom correspondence should be addressed at Department of Chemistry and Biotechnology, School of Engineering, The University of Tokyo, Hongo, Tokyo 113-8656, Japan. Tel: +81 3 5841 8828 or +81 29 861 3015; Fax: +81 29 861 3019; Email: taira@chembio.t.u-tokyo.ac.jp

The authors wish it to be known that, in their opinion, the first two authors should be regarded as joint First Authors

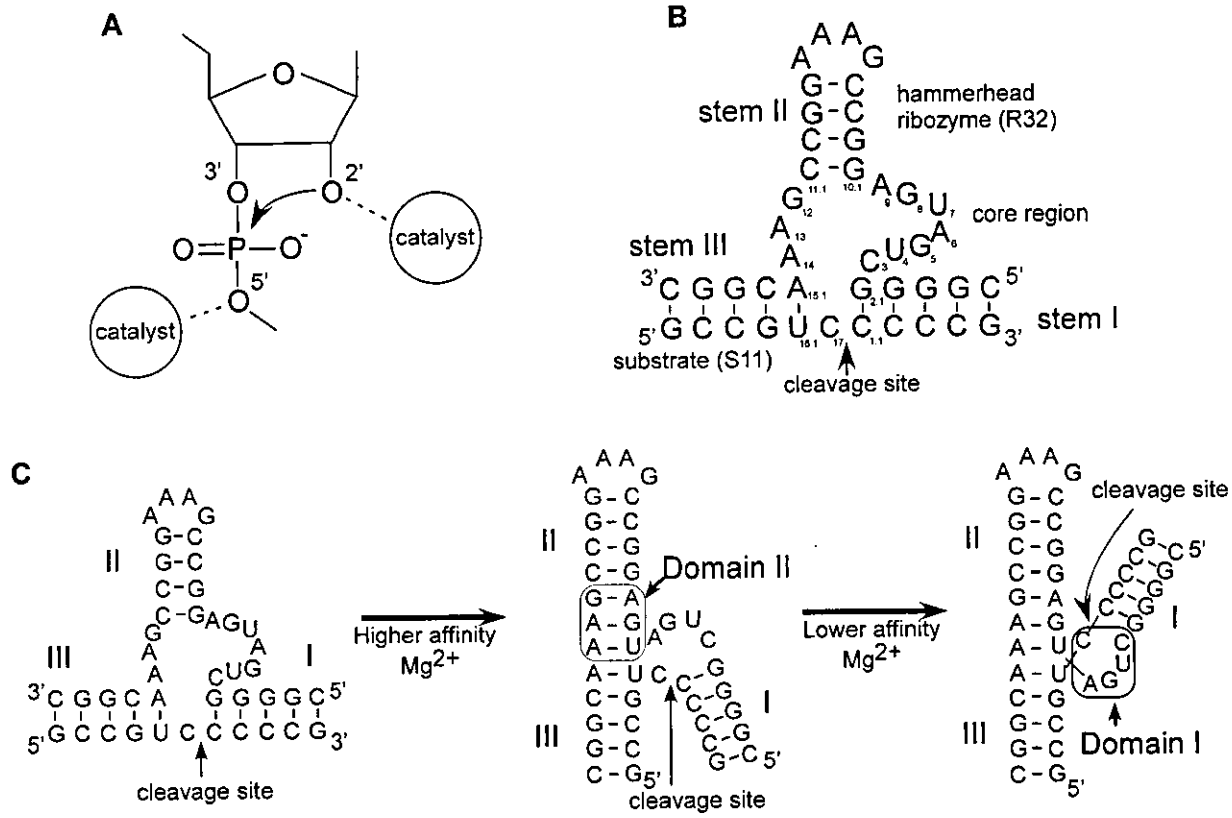

Figure 1. (**A**) Schematic representation of the proposed mechanism of the hammerhead ribozyme reaction. The 2′-hydroxyl moiety is activated by the catalyst and attacks the adjacent phosphate nucleophilically, with subsequent cleavage of the bond at the 5′-oxygen. The developing negative charge on the leaving 5′-oxygen is stabilized by another catalyst. (**B**) The sequences and secondary structures of the hammerhead ribozyme (R32) and substrate (S11) used in this study. (**C**) The proposed two-stage folding scheme for the hammerhead ribozyme–substrate complex. The higher-affinity Mg^{2+} ion(s) drives the formation of domain II, which contains non-Watson–Crick pairings and the lower-affinity Mg^{2+} ion(s) rotates around helix I, forming the catalytic core.

to physiological concentrations, is useful for studies of the chemistry of the hammerhead ribozyme and it allowed us to estimate the intrinsic cleavage rate constant and to compare an enzymatic reaction to a non-enzymatic reaction. We were also able to calculate acceleration energy more precisely and to investigate the dependence on Mg^{2+} ions in the presence of high concentrations of Li^{+} ions. Considering the results of such analyses, we propose the existence of a new cooperative pathway that involves divalent metal ions, such as Mg^{2+}, and monovalent ions, such as Li^{+}, in the reaction catalyzed by a hammerhead ribozyme. We also discuss the nature of the catalysts.

MATERIALS AND METHODS

Preparation of the hammerhead ribozyme and its substrate

The ribozyme (R32) and its substrate (S11) were synthesized chemically on a DNA/RNA synthesizer (model 394; PE Applied Biosystems, Foster City, CA) using phosphoramidic chemistry with 2′-*tert* butyldimethylsilyl (TBDMS) protection as described previously (25). Chemically synthesized oligonucleotides were deprotected in a mixture of 28% ammonia and ethanol (3:1) at 55°C for 8 h. The mixture was evaporated to dryness and the residue was allowed to dissolve in 1 ml of 1 M tetrabutylammonium fluoride (TBAF; Sigma-Aldrich, Japan K.K., Tokyo, Japan) at room temperature for 12 h. After the addition of 1 ml of water, the mixture was desalted on a gel-filtration column (Bio-Gel P-4; Bio-Rad Laboratories, Hercules, CA). Fully deprotected oligonucleotides were purified by gel electrophoresis on a 20% polyacrylamide gel that contained 7 M urea, the respective bands were excised from the gel, and oligonucleotides were extracted in water. The oligonucleotides were recovered by ethanol precipitation and then solutions were desalted on a gel-filtration column (TSK-GEL G3000PW; TOSOH, Tokyo, Japan) by high-performance liquid chromatography (HPLC) with ultrapure water. All of the RNA oligomers were quantitated in terms of absorbance at 260 nm.

The substrate S11 was labeled with [γ-^{32}P]ATP by T4 polynucleotide kinase (Takara Bio, Inc., Shiga, Japan). Radiolabeled S11 was purified on a 20% polyacrylamide gel that contained 7 M urea and then purified by the standard procedure, as described above, with desalting on a gel-filtration column (NAP^{TM}-10 column; Amersham Biosciences, K.K., Tokyo, Japan).

Quantification of the ribozyme reaction

All ribozyme reactions were performed under single-turnover conditions to ensure that conversion of the ribozyme–substrate

complex to the ribozyme–product complex could be monitored kinetically without complications due to complex formation and slow release of products. The solution for the ribozyme reaction contained a trace amount of 5′-^{32}P-labeled S11 and 25 mM Bis-Tris buffer at pH 6.0 and 25°C. The pH values of all 1.25× pre-stock Bis-Tris buffers that contained appropriate metal ions (metal-ion–buffer) were adjusted appropriately with HCl and we confirmed that each buffer had the appropriate pH under the chosen reaction conditions. Each reaction was initiated by addition of the substrate to a mixture of metal-ion–buffer and ribozyme, and aliquots were removed from the reaction mixture at appropriate intervals. Each aliquot was mixed with more than three volumes of a stop solution that contained 100 mM MES (pH 6), 100 mM EDTA, 7 M urea, xylene cyanol (0.1%) and bromophenol blue (0.1%), and then it was stored at −80°C prior to analysis. Since EDTA does not chelate Mg^{2+} and Li^+ ions efficiently at lower pH values, we confirmed that reactions did not continue in the stop solution and that quenching was effective due to high concentration of urea in this solution. Uncleaved substrate and 5′-cleaved products were separated on a 20% polyacrylamide gel that contained 7 M urea. The extent of each cleavage reaction was quantitated with an imageanalyzer (Storm 830; Molecular Dynamics, Sunnyvale, CA). For each reaction, an observed rate constant was determined by non-linear least-squares fitting of the time course of reaction using a pseudo-first-order equation.

RESULTS AND DISCUSSION

The dependence of the activity of the hammerhead ribozyme on the concentration of Li^+ ions

We examined the dependence of the activity of the ribozyme on the concentration of Li^+ ions to confirm that Li^+ ions affect the ribozyme's activity, as reported previously by others (51). We performed reactions under single-turnover conditions at pH 7.5 and 25°C. The results are shown in Figure 2A. Although the activity reached a plateau at ~3 M Li^+ ions, the dependence on the concentration of Li^+ ions was observed (with a slope of three) below the plateau. In the study by O'Rear *et al.* (51), the hammerhead ribozyme reaction exhibited second-order dependence on Li^+ ions up to 4 M at pH 7.5. Although our curve is steeper than the curve that they obtained under the same conditions, with the exception of the concentrations of Li^+ ions, the slopes of both profiles obtained with Li^+ ions are clearly steeper than those of profiles obtained with Mg^{2+} ions. Our profile is unique insofar as we observed saturation of the ribozyme reaction in the range of 3–5 M (Figure 2A). This plateau suggests that the ribozyme reaction might involve the binding of Li^+ ions to the ribozyme–substrate complex.

We also confirmed the dependence on pH, with a slope of unity, of the activity in the presence of a high concentration of Li^+ ions, as shown in Figure 2B. This result supports the hypothesis that the cleavage step is the rate-limiting step even at such a high ionic strength. The pH profile is also consistent with the previous report by Curtis and Bartel (52). As shown in Figure 2A, the observed rate constant at a saturating concentration of Li^+ ions (3–5 M) at pH 7.5 was ~0.17 min^{-1}. The estimated observed rate constant in the

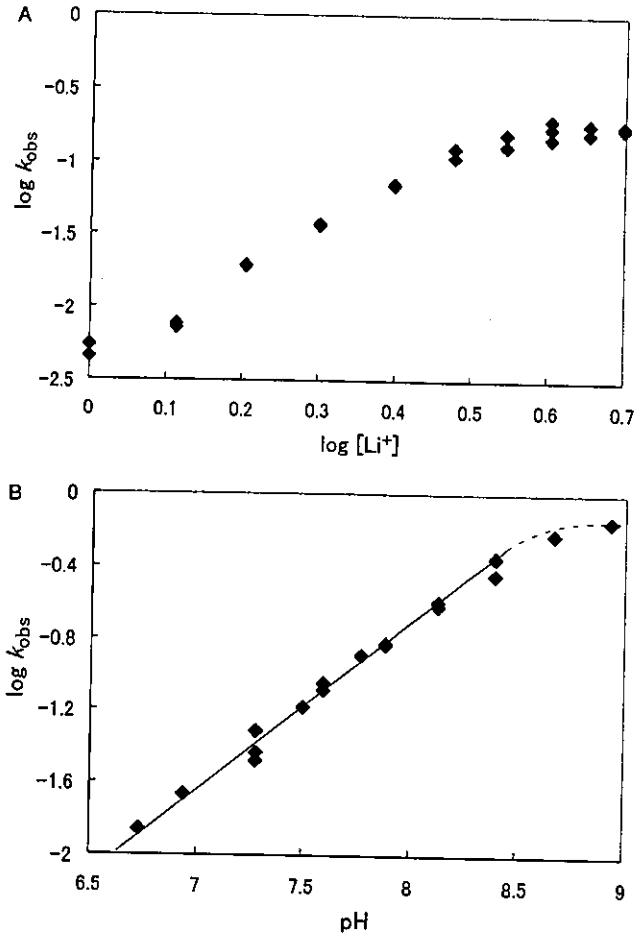

Figure 2. (**A**) Dependence of cleavage activity on the concentration of Li^+ ions. The activity increased linearly with the concentration of Li^+ ions until ~3 M. Reaction conditions: 25 mM Bis-Tris, pH 7.5, and varying concentrations of Li^+ ions as indicated. (**B**) Dependence on pH of the activity in 2 M Li^+ ions. The Li^+-containing buffer used in this experiment included Bis-Tris propane and Tris. The cleavage rate increased linearly with pH, yielding a slope of 0.9.

presence of 800 mM Mg^{2+} ions was 32 min^{-1} at pH 7.5, as determined from the value of 1 min^{-1} at pH 6 at the same temperature as that at which the Li^+ experiment was performed (see later). The difference was, thus, approximately 200-fold under similar conditions. The true difference might be even greater because, in contrast to the results with Li^+, the rate at 800 mM Mg^{2+} does not reach a plateau value (see later). These data indicate clearly that Mg^{2+} ions are more suitable for an effective hammerhead ribozyme reaction than any other monovalent ions (Li^+ ions have the highest activity of all monovalent ions in the ribozyme reaction).

The dependence of the activity of the hammerhead ribozyme on the concentration of Mg^{2+} ions

We attempted first to determine how many Mg^{2+} ions might be involved in our model ribozyme reaction and the saturating concentration of Mg^{2+} ions in the reaction, beyond which the cleavage rate constant no longer increases. We examined the dependence on the concentration of Mg^{2+} ions of the activity

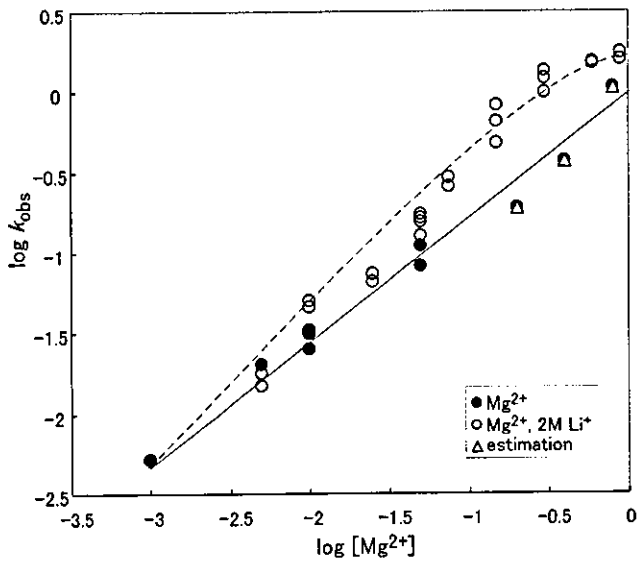

Figure 3. The Mg^{2+}-titration curve for cleavage activity in the presence (open circles) and absence (filled circles) of Li^+ ions. In the absence of Li^+ ions, the line drawn with the linear best fit had a slope of 0.7. The activity increased with increasing concentrations of Mg^{2+} ions and did not reach a plateau value even at 800 mM Mg^{2+} ions. In the presence of 2 M Li^+ ions, the activity increased with increases in the concentration of Mg^{2+} ions up to ~600 mM. Triangles are the calculated rates in the presence of Mg^{2+} ions plus 2 M Li^+ ions, which were determined simply by adding the respective reaction rates together. Since the observed rate in the presence of 2 M Li^+ ions only at pH 6 was <0.01 min^{-1}, triangles are at almost the same positions as the filled circles. The rates observed in the presence of Mg^{2+} ions and Li^+ ions together (open circles) were clearly higher than the calculated values (triangles).

of the R32 hammerhead ribozyme up to ~1 M Mg^{2+} ions. We performed reactions with R32-S11 (Figure 1B) under single-turnover conditions with a saturating amount of ribozyme with respect to the amount of S11 for the same reasons as noted above. The reaction in the presence of Mg^{2+} ions is accelerated with increases in pH, with a slope of unity (7,40,43,44,47,53). We adjusted the pH of reactions to 6.0 to slow down the reaction so that we could determine the rate constants of rapid reactions precisely. As shown by closed circles in Figure 3, the dependence on Mg^{2+} ions was approximately first-order. However, no plateau was reached under our conditions, even above 800 mM Mg^{2+} ions. The continuous increase in rate constant upon the addition of more and more Mg^{2+} ions indicates the involvement of one Mg^{2+} ion that has low affinity for the hammerhead ribozyme–substrate complex. At 800 mM Mg^{2+} ions, the rate constant approached 1.1 min^{-1} at pH 6.0, and this is the limit of detection of a rapid cleavage reaction under standard laboratory conditions.

Analyses of the structure of hammerhead ribozymes and of the conformational changes caused by interactions with Mg^{2+} ions have indicated that two major conformational changes occur: the formation of domain II, which is followed by the formation of domain I, as shown in Figure 1C (38,45, 48,50,54). The formation of domain II results in coaxial stacking of helices II and III, induced by the binding of a higher-affinity Mg^{2+} ion(s) to P9 phosphate and N7 of $G_{10.1}$ (P9/G10.1) of the ribozyme–substrate complex (38,45,48,50,54–58). The second transition is the formation of the catalytic domain with movement of stem I toward stem II, which is induced by the binding of a lower-affinity Mg^{2+} ion(s). The K_d values of the two domains have been determined by various methods to be several hundred micromolar and several millimolar, respectively (45,46,48,50,54). Thus, at several hundred millimolar Mg^{2+} ions, the formation of domains II and I should be complete.

Taking this structural information into consideration, we can reasonably conclude that the very-low-affinity Mg^{2+} ion that we detected in the present study might be involved in some step other than the formation of domains I and II. This step might be a conformational change or the binding of a catalytic species to the ribozyme–substrate complex. Walter and coworkers recently reported that a third and previously undetected metal ion at rather high concentrations might play a role in the induction of a minor conformational adjustment that leads to the formation of the active state after the formation of domains I and II (59). The Mg^{2+} ion that we detected had very low affinity, and the relative level of truly active ribozyme species at a concentration of several millimolar Mg^{2+} ions corresponded to <1% of all the ribozyme–substrate complexes in the reaction mixture [compare 1 min^{-1} in 10 mM $MgCl_2$ at pH 8 and 25°C (60) with 100 min^{-1} in 800 mM $MgCl_2$ at the same pH and the same temperature (see later)].

One might agree that Figure 3 does not support the existence of a very-low-affinity binding site for an Mg^{2+} ion on the ribozyme–substrate complex since the binding curve does not reach a plateau. If the dependence that we observed here were due only to ionic strength, no plateau would be observed. However, we did observe a plateau in the case of Li^+ ions (Figure 2A). Because reactions were so rapid, even at low pH, we could not monitor the kinetics at even higher concentrations of Mg^{2+} ions, such as 3 M. However, it is likely that, in ribozyme reactions, ionic strength is less important than the ion radius and/or the electron density of metal ions since (i) a correlation between the ion radius of Group I monovalent metal ions and ribozyme activity has been observed (52,57) and (ii) an apparent plateau was reached in the presence of high concentrations of Mg^{2+} ions plus 2 M Li^+ ions (Figure 3). Although we cannot calculate a Hill constant for Mg^{2+} ions and estimate the number of binding sites for Mg^{2+} ions from our current data, all the available data strongly support the possibility of the existence of a very-low-affinity metal-binding site(s).

Misra and Draper (61) proposed a model for the stabilization of RNA by Mg^{2+} ions that arises from two distinct binding modes, diffuse binding and site binding. Diffusely bound Mg^{2+} ions are defined as fully solvated ions that interact with RNA only through long-range electrostatic interactions. Site-bound Mg^{2+} ions are defined as partially desolvated ions that are attracted to electronegative pockets. In general, the affinity of diffusely bound Mg^{2+} ions appears to be lower than that of site-bound Mg^{2+} ions. Thus, it is possible that the very-low-affinity Mg^{2+} ions that we detected here might be involved in diffuse binding. Although diffuse binding can sometimes play a dominant role in stabilizing the tertiary structures of small RNAs (61), we cannot exclude the possibility that such diffuse binding Mg^{2+} ion might play a role in catalysis in the ribozyme reaction at a specific site in the ribozyme–substrate complex.

In 800 mM Mg^{2+} ions, the observed rate constant of the reaction catalyzed by the hammerhead ribozyme can be estimated to be ~100 min^{-1} at pH 8 and 25°C, from the

dependence on pH with a slope of unity. The estimated rate constant at concentrations of Mg^{2+} ions >800 mM should be much higher than that at 800 mM since the cleavage reaction did not reach saturation at 800 mM Mg^{2+} and approached the estimated observed rate constant of a 'kissing ribozyme', under saturating conditions with respect to Mg^{2+} ions and pH (62).

The dependence of the activity of the hammerhead ribozyme on Mg^{2+} ions in the presence of a high concentration of Li^+ ions

In order to investigate the properties of Mg^{2+} ions in the ribozyme reaction in further detail, we examined the dependence on Mg^{2+} ions in the presence of a high concentration (2 M) of Li^+ ions. We chose the Li^+ ion as the monovalent cation because this ion is the most active of a large variety of monovalent cations (57). At 2 M Li^+ ions at pH 6.0, the hammerhead ribozyme had detectable activity in the absence of Mg^{2+} ions. We varied the concentration of Mg^{2+} ions from 5 to 900 mM and measured the rate constant. As shown by open circles in Figure 3, we observed approximately first-order dependence on the concentration of Mg^{2+} ions up to 600 mM, and then the rate constant started to reach a plateau from 600 to 900 mM Mg^{2+} ions. These data indicate that, even in the presence of a very high concentration of Li^+ ions, an Mg^{2+} ion with very low affinity plays an important role in the hammerhead ribozyme reaction. The plateau that seemed to appear in the presence of high concentrations of Li^+ ions (Figure 3, open circles) was not observed in the absence of Li^+ ions (closed circles). This apparent plateau was not due to misfolding of RNA at such a high ionic concentration because the extent of cleavage at the end of the reaction was always >90% under these conditions. The plateau might indicate that Li^+ ions help the ribozyme–substrate complex to fold into a more active form, contributing to the enhanced binding of the very-low-affinity Mg^{2+} ion(s) to the complex.

We examined reactions in the presence of Mg^{2+} ions only (Figure 3, closed circles) and in the presence of Li^+ ions only (57). We then calculated rate constants (Figure 3, triangles) on the assumption that Mg^{2+} and Li^+ ions function independently. It should be noted that the observed rate constant in the presence of both Mg^{2+} ions and 2 M Li^+ ions together (Figure 3, open circles) was definitely higher than the calculated rates (Figure 3, triangles) at pH 6 (compare open circles with triangles in Figure 3). One might expect that, in such an experiment (i) the activities in the presence of both metal ions together would be lower than the estimated activities (triangles) because of the lower ability of Mg^{2+} ions to bind to RNA in the presence of high ionic strength due to 2 M Li^+ ions and (ii) the stimulation by Mg^{2+} ions in the presence of such a high concentration of Li^+ ions would be smaller than in the absence of Li^+ ions. It has been reported that stimulation by Cd^{2+} ions is reduced in a ribozyme reaction in the presence of 4 M Li^+ ions (51), while stimulation by Cd^{2+} ions is observed in reaction mixtures that contain 10 mM Ca^{2+} ions instead of 2 M Li^+ ions (23). However, the results in the present study were quite opposite: (i) the activities in the presence of Mg^{2+} ions and 2 M Li^+ ions together (open circles in Figure 3) were higher than the calculated activities (triangles in Figure 3), and (ii) the stimulation by Mg^{2+} ions in the presence of 2 M Li^+ ions (open circles in Figure 3) was even greater than that by Mg^{2+} ions in the absence of Li^+ ions (closed circles in Figure 3).

Our observations suggest the existence of a new cooperative pathway that involves Li^+ and Mg^{2+} ions, in which both metal ions function cooperatively in structural support and/or as the catalyst(s) to increase the rate constant of cleavage (57). In the case of cleavage of RNA by another type of ribozyme, the RNA subunit of RNase P, a similar cooperativity between the metal ions, e.g. Mg^{2+} and Ca^{2+}, has been reported (63).

What is the catalyst in the hammerhead reaction?

To the best of our knowledge, this report is the first to describe the dependence of ribozyme activity on a high concentration of Mg^{2+} ions under single-turnover conditions (Figure 3). The reaction did not reach a plateau even at 800 mM Mg^{2+} ions. Under these conditions at pH 6, the observed rate constant was 1.1 min^{-1}. The activity of the ribozyme is known to depend on pH, with a slope of unity. Thus, we can estimate an observed rate constant for the ribozyme reaction of 110 min^{-1} at pH 8. It is very unlikely that this rate constant of cleavage can occur without an effective catalyst(s) (64). So, what is the catalyst(s) of the reaction?

In studies of solvent isotope effects on the ribozyme reaction in the presence of deuterium and Li^+, Mg^{2+} or NH_4^+ ions, we failed previously to observe any proton transfers in the transition state during the ribozyme reaction in the presence of either Li^+ or Mg^{2+} ions but we did observe proton transfer in the presence of NH_4^+ ions (53,65). We interpreted such results by suggesting that metal ions, such as Mg^{2+} and Li^+, function as a Lewis acid catalyst while NH_4^+ ions function as a general acid catalyst during the ribozyme reaction. Thus, the catalyst can change according to the conditions around the ribozyme. On the basis of this hypothesis and the involvement of two other kinds of Mg^{2+} ions in the formation of domains I and II, it is possible that the newly identified Mg^{2+} ion with very low affinity that we observed in this study might be the true catalyst. Our novel cooperative pathway might involve an Mg^{2+} ion in a catalytic role after monovalent cations and other Mg^{2+} ions have acted to generate the pre-active conformation just before chemical cleavage by the hammerhead ribozyme. In the presence of monovalent ions exclusively, monovalent ions can also function as the catalyst but they are not as effective. Mg^{2+} ions have a higher charge density than Li^+ ions and would function better as catalyst in the reaction. Thus, when both Mg^{2+} and Li^+ ions are present in the reaction mixture, the high activity of the ribozyme reaction is likely due to an Mg^{2+} ion catalyst. The Li^+ ions act to support the formation of the domains I and II in cooperation with Mg^{2+} ions, as discussed above.

We are at present constructing a reaction scheme for ribozyme reactions in the presence of both Mg^{2+} and Li^+ ions, namely, a 'cooperative pathway', by determining the details of the stoichiometric relationships among these metal ions (57). Examination of ribozyme-catalyzed reactions in the presence of various metal ions in combination should clarify the roles of metal ions in catalysis.

ACKNOWLEDGEMENTS

The authors thank Dr Laura Nelson for helpful comments.

REFERENCES

1. Cech,T.R., Zaug,A.J. and Grabowski,P.J. (1981) *In vitro* splicing of the ribosomal RNA precursor of *Tetrahymena*: involvement of a guanosine nucleotide in the excision of the intervening sequence. *Cell*, **27**, 487–496.
2. Guerrier-Takada,C., Gardiner,K., Marsh,T., Pace,N. and Altman,S. (1983) The RNA moiety of ribonuclease P is the catalytic subunit of the enzyme. *Cell*, **35**, 849–857.
3. Symons,R.H. (1992) Small catalytic RNAs. *Annu. Rev. Biochem.*, **61**, 641–671.
4. Carola,C. and Eckstein,F. (1999) Nucleic acid enzymes. *Curr. Opin. Chem. Biol.*, **3**, 274–283.
5. Warashina,M., Zhou,D.M., Kuwabara,T. and Taira,K. (1999) Ribozyme structure and function. In Söll,D., Nishimura,S. and Moore,P.B. (eds), *Comprehensive Natural Products Chemistry*. Elsevier Science Ltd, Oxford, Vol. 6, pp. 235–268.
6. Warashina,M., Takagi,Y., Stec,W.J. and Taira,K. (2000) Differences among mechanisms of ribozyme-catalyzed reactions. *Curr. Opin. Biotechnol.*, **11**, 354–362.
7. Takagi,Y., Warashina,M., Stec,W.J., Yoshinari,K. and Taira,K. (2001) Recent advances in the elucidation of the mechanisms of action of ribozymes. *Nucleic Acids Res.*, **29**, 1815–1834.
8. Noller,H.F., Hoffarth,V. and Zimniak,L. (1992) Unusual resistance of peptidyl transferase to protein extraction procedures. *Science*, **256**, 1416–1419.
9. Nissen,P., Hansen,J., Ban,N., Moore,P.B. and Steitz,T.A. (2000) The structural basis of ribosome activity in peptide bond synthesis. *Science*, **289**, 920–930.
10. Muth,G.W., Ortoleva-Donnelly,L. and Strobel,S.A. (2000) A single adenosine with a neutral pK_a in the ribosomal peptidyl transferase center. *Science*, **289**, 947–950.
11. Cech,T.R. (2000) Structural biology. The ribosome is a ribozyme. *Science*, **289**, 878–879.
12. Collins,C.A. and Guthrie,C. (2000) The question remains: is the spliceosome a ribozyme? *Nature Struct. Biol.*, **10**, 850–854.
13. Hampel,A. and Cowan,J.A. (1997) A unique mechanism for RNA catalysis: the role of metal cofactors in hairpin ribozyme cleavage. *Chem. Biol.*, **4**, 513–517.
14. Nesbitt,S., Hegg,L.A. and Fedor,M.J. (1997) An unusual pH-independent and metal-ion-independent mechanism for hairpin ribozyme catalysis. *Chem. Biol.*, **4**, 619–630.
15. Young,K.J., Gill,F. and Grasby,J.A. (1997) Metal ions play a passive role in the hairpin ribozyme catalysed reaction. *Nucleic Acids Res.*, **25**, 3760–3766.
16. Chowrira,B.M., Berzal-Herranz,A. and Burke,J.M. (1993) Ionic requirements for RNA binding, cleavage, and ligation by the hairpin ribozyme. *Biochemistry*, **32**, 1088–1095.
17. Earnshaw,D.J. and Gait,M.J. (1998) Hairpin ribozyme cleavage catalyzed by aminoglycoside antibiotics and the polyamine spermine in the absence of metal ions. *Nucleic Acids Res.*, **26**, 5551–5561.
18. Seyhan,A.A. and Burke,J.M. (2000) Mg^{2+}-independent hairpin ribozyme catalysis in hydrated RNA films. *RNA*, **6**, 189–198.
19. Uhlenbeck,O.C. (1987) A small catalytic oligoribonucleotide. *Nature*, **328**, 596–600.
20. Haseloff,J. and Gerlach,W.L. (1988) Simple RNA enzymes with new and highly specific endoribonuclease activities. *Nature*, **334**, 585–591.
21. Hutchins,C.J., Rathjen,P.D., Forster,A.C. and Symons,R.H. (1986) Self-cleavage of plus and minus RNA transcripts of avocado sunblotch viroid. *Nucleic Acids Res.*, **14**, 3627–3640.
22. Koizumi,M., Hayase,Y., Iwai,S., Kamiya,H., Inoue,H. and Ohtsuka,E. (1989) Design of RNA enzymes distinguishing a single base mutation in RNA. *Nucleic Acids Res.*, **17**, 7059–7071.
23. Wang,S., Karbstein,K., Peracchi,A., Beigelman,L. and Herschlag,D. (1999) Identification of the hammerhead ribozyme metal ion binding site responsible for rescue of the deleterious effect of a cleavage site phosphorothioate. *Biochemistry*, **38**, 14363–14378.
24. Maderia,M., Hunsicker,L.M. and DeRose,V.J. (2000) Metal–phosphate interactions in the hammerhead ribozyme observed by ^{31}P NMR and phosphorothioate substitutions. *Biochemistry*, **39**, 12113–12120.
25. Yoshinari,K. and Taira,K. (2000) A further investigation and reappraisal of the thio effect in the cleavage reaction catalyzed by a hammerhead ribozyme. *Nucleic Acids Res.*, **28**, 1730–1742.
26. Peracchi,A., Beigelman,L., Scott,E.C., Uhlenbeck,O.C. and Herschlag,D. (1997) Involvement of a specific metal ion in the transition of the hammerhead ribozyme to its catalytic conformation. *J. Biol. Chem.*, **272**, 26822–26826.
27. Knöll,R., Bald,R. and Fürste,J.P. (1997) Complete identification of nonbridging phosphate oxygens involved in hammerhead cleavage. *RNA*, **3**, 132–140.
28. Nakamatsu,Y., Warashina,M., Kuwabara,T., Tanaka,Y., Yoshinari,K. and Taira,K. (2000) Significant activity of a modified ribozyme with N7-deazaguanine at $G_{10.1}$: the double-metal-ion mechanism of catalysis in reactions catalysed by hammerhead ribozymes. *Genes Cells*, **5**, 603–612.
29. Peracchi,A., Beigelman,L., Usman,N. and Herschlag,D. (1996) Rescue of abasic hammerhead ribozymes by exogenous addition of specific bases. *Proc. Natl Acad. Sci. USA*, **93**, 11522–11527.
30. Peracchi,A., Karpeisky,A., Maloney,L., Beigelman,L. and Herschlag,D. (1998) A core folding model for catalysis by the hammerhead ribozyme accounts for its extraordinary sensitivity to abasic mutations. *Biochemistry*, **37**, 14765–14775.
31. Murray,J.B. and Scott,W.G. (2000) Does a single metal ion bridge the A-9 and scissile phosphate groups in the catalytically active hammerhead ribozyme structure? *J. Mol. Biol.*, **296**, 33–41.
32. Tanaka,Y., Morita,E.H., Hayashi,H., Kasai,Y., Tanaka,T. and Taira,K. (2000) Well-conserved tandem G•A pairs and the flanking C•G pair in hammerhead ribozymes are sufficient for capture of structurally and catalytically important metal ions. *J. Am. Chem. Soc.*, **122**, 11303–11310.
33. Suzumura,K., Warashina,M., Yoshinari,K., Tanaka,Y., Kuwabara,T., Orita,M. and Taira,K. (2000) Significant change in the structure of a ribozyme upon introduction of a phosphorothioate linkage at P9: NMR reveals a conformational fluctuation in the core region of a hammerhead ribozyme. *FEBS Lett.*, **473**, 106–112.
34. Tanaka,Y., Kojima,C., Morita,E.H., Kasai,K., Ono,A., Kainosho,M. and Taira,K. (2002) Identification of the metal ion binding site on an RNA motif from hammerhead ribozymes using ^{15}N-NMR spectroscopy. *J. Am. Chem. Soc.*, **124**, 4595–4601.
35. Hansen,M.R., Simorre,J.P., Hanson,P., Mokler,V., Bellon,L., Beigelman,L. and Pardi,A. (1999) Identification and characterization of a novel high affinity metal-binding site in the hammerhead ribozyme. *RNA*, **5**, 1099–1104.
36. Feig,A.L., Panek,M., Horrocks,W.D. and Uhlenbeck,O.C. (1999) Probing the binding of Tb(III) and Eu(III) to the hammerhead ribozyme using luminescence spectroscopy. *Chem. Biol.*, **6**, 801–810.
37. Murray,J.B., Seyhan,A.A., Walter,N.G., Burke,J.M. and Scott,W.G. (1998) The hammerhead, hairpin and VS ribozymes are catalytically proficient in monovalent cations alone. *Chem. Biol.*, **5**, 587–595.
38. Zhou,J.-M., Zhou,D.-M., Takagi,Y., Kasai,Y., Inoue,A., Baba,T. and Taira,K. (2002) Existence of efficient divalent metal ion-catalyzed and inefficient divalent metal ion-independent channels in reactions catalyzed by a hammerhead ribozyme. *Nucleic Acids Res.*, **30**, 2374–2382.
39. Kasai,Y., Shizuku,H., Takagi,Y., Warashina,M. and Taira,K. (2002) Measurements of weak interactions between truncated substrates and a hammerhead ribozyme by competitive kinetic analyses: implications for the design of new and efficient ribozymes with high sequence specificity. *Nucleic Acids Res.*, **30**, 2383–2389.
40. Zhou,D.-M. and Taira,K. (1998) The hydrolysis of RNA: from theoretical calculations to the hammerhead ribozyme-mediated cleavage of RNA. *Chem. Rev.*, **98**, 991–1026.
41. Takagi,Y. and Taira,K. (1995) Temperature-dependent change in the rate-determining step in a reaction catalyzed by a hammerhead ribozyme. *FEBS Lett.*, **361**, 273–276.
42. Koizumi,M. and Ohtsuka,E. (1991) Effects of phosphorothioate and 2-amino groups in hammerhead ribozymes on cleavage rates and Mg^{2+} binding. *Biochemistry*, **30**, 5145–5150.
43. Dahm,S.C., Derrick,W.B. and Uhlenbeck,O.C. (1993) Evidence for the role of solvated metal hydroxide in the hammerhead cleavage mechanism. *Biochemistry*, **32**, 13040–13045.
44. Hendry,P. and McCall,M.J. (1995) A comparison of the *in vitro* activity of DNA-armed and all-RNA hammerhead ribozymes. *Nucleic Acids Res.*, **23**, 3928–3936.
45. Bassi,G.S., Murchie,A.I.H., Walter,F., Clegg,R.M. and Lilley,D.M.J. (1997) Ion-induced folding of the hammerhead ribozyme: a fluorescence resonance energy transfer study. *EMBO J.*, **16**, 7481–7489.
46. Horton,T.E., Clardy,D.R. and DeRose,V.J. (1998) Electron paramagnetic resonance spectroscopic measurement of Mn^{2+} binding affinities to the hammerhead ribozyme and correlation with cleavage activity. *Biochemistry*, **37**, 18094–18101.

47. Peracchi,A. (1999) Origins of the temperature dependence of hammerhead ribozyme catalysis. *Nucleic Acids Res.*, **27**, 2875–2882.
48. Bassi,G.S., Møllegaard,N.E., Murchie,A.I.H. and Lilley,D.M.J. (1999) RNA folding and misfolding of the hammerhead ribozyme. *Biochemistry*, **38**, 3345–3354.
49. Hunsicker,L.M. and DeRose,V.J. (2000) Activities and relative affinities of divalent metals in unmodified and phosphorothioate-substituted hammerhead ribozymes. *J. Inorg. Biochem.*, **80**, 271–281.
50. Hammann,C., Norman,D.G. and Lilley,D.M.J. (2001) Dissection of the ion-induced folding of the hammerhead ribozyme using ^{19}F-NMR. *Proc. Natl Acad. Sci. USA*, **98**, 5503–5508.
51. O'Rear,J.L., Wang,S., Feig,A.L., Beigelman,L., Uhlenbeck,O.C. and Herschlag,D. (2001) Comparison of the hammerhead cleavage reactions stimulated by monovalent and divalent cations. *RNA*, **7**, 537–545.
52. Curtis,E.A. and Bartel,D.P. (2001) The hammerhead cleavage reaction in monovalent cations. *RNA*, **7**, 546–552.
53. Takagi,Y. and Taira,K. (2002) Detection of a proton-transfer process by kinetic solvent isotope effects in NH_4^+-mediated reactions catalyzed by a hammerhead ribozyme. *J. Am. Chem. Soc.*, **124**, 3850–3852.
54. Bassi,G.S., Møllegaard,N.E., Murchie,A.I.H., von Kitzing,E. and Lilley,D.M.J. (1995) Ionic interactions and the global conformations of the hammerhead ribozyme. *Nature Struct. Biol.*, **2**, 45–55.
55. Schiemann,O., Fritscher,J., Kisseleva,N., Sigurdsson,S.T. and Prisner,T.F. (2003) Structural investigation of a high-affinity MnII binding site in the hammerhead ribozyme by EPR spectroscopy and DFT calculations. Effects of neomycin B on metal-ion binding. *ChemBioChem*, **4**, 1057–1065.
56. Tanaka,Y., Kasai,Y., Mochizuki,S., Wakisaka,A., Morita,E.H., Kojima,C., Toyozawa,A., Kondo,Y., Taki,M., Takagi,Y., Inoue,A., Yamasaki,K. and Taira,K. (2004). Nature of the chemical bond formed with the structural metal ion at the A9/G10.1 motif derived from hammerhead ribozymes. *J. Am. Chem. Soc.*, **126**, 744–752.
57. Takagi,Y., Inoue,A. and Taira,K. (2004). Analysis of on a cooperative pathway involving multiple cations in hammerhead reactions. *J. Am. Chem. Soc.*, in press.
58. Warashina,M., Kuwabara,T., Nakamatsu,Y., Takagi,Y., Kato,Y. and Taira,K. (2004) Analysis of the conserved P9-G10.1 metal binding motif in hammerhead ribozymes with extra nucleotide inserted between A9 and G10.1 residues. *J. Am. Chem. Soc.*, in press.
59. Rueda,D., Wick,K., McDowell,S.E. and Walter,N.G. (2003) Diffusely bound Mg^{2+} ions slightly reorient stems I and II of the hammerhead ribozyme to increase the probability of formation of the catalytic core. *Biochemistry*, **42**, 9924–9936.
60. Stage-Zimmermann,T.K. and Uhlenbeck,O.C. (1998) Hammerhead ribozyme kinetics. *RNA*, **4**, 875–889.
61. Misra,V.K. and Draper,D.E. (2002) The linkage between magnesium binding and RNA folding. *J. Mol. Biol.*, **317**, 507–521.
62. Khvorova,A., Lescoute,A., Westhof,E. and Jayasena,S.D. (2003) Sequence elements outside the hammerhead ribozyme catalytic core enable intracellular activity. *Nature Struct. Biol.*, **10**, 708–712.
63. Brännvall,M. and Kirsebom,L.A. (2001) Metal ion cooperativity in ribozyme cleavage of RNA. *Proc. Natl Acad. Sci. USA*, **98**, 12943–12947.
64. Li,Y. and Breaker,R.R. (1999) Kinetics of RNA degradation by specific base catalysis of transesterification involving the 2′-hydroxyl group. *J. Am. Chem. Soc.*, **121**, 5364–5372.
65. Sawata,S., Komiyama,M. and Taira,K. (1995) Kinetic evidence based on solvent isotope effects for the nonexistence of a proton-transfer process in reactions catalyzed by a hammerhead ribozyme—implication to the double-metal-ion mechanism of catalysis. *J. Am. Chem. Soc.*, **117**, 2357–2358.

Accelerated Publication

THE JOURNAL OF BIOLOGICAL CHEMISTRY
Vol. 279, No. 37, Issue of September 10, pp. 38083–38086, 2004

Identification of Metastasis-related Genes in a Mouse Model Using a Library of Randomized Ribozymes*

Received for publication, July 1, 2004
Published, JBC Papers in Press, July 9, 2004,
DOI 10.1074/jbc.C400313200

Eigo Suyama‡§¶, Renu Wadhwa§¶, Kamaljit Kaur§, Makoto Miyagishi‡§, Sunil C. Kaul§, Hiroaki Kawasaki‡§, and Kazunari Taira‡§‖

From the ‡Department of Chemistry and Biotechnology, School of Engineering, The University of Tokyo, 7-3-1 Hongo, Bunkyo-ku, Tokyo 113-8656, Japan and the §Gene Function Research Center, National Institute of Advanced Industrial Science and Technology (AIST), Central 4, 1-1-1 Higashi, Tsukuba Science City, Ibaraki 305-8562, Japan

Libraries of randomized ribozymes have considerable potential as tools for the identification of functional genes critically involved in a biological phenotype of interest *in vitro*. We have used a ribozyme library in an *in vivo* mouse model to identify genes related to metastasis. We injected weakly metastatic melanoma cells that had been treated with the library intravenously into mice. We then isolated ribozymes that accelerated metastasis from pulmonary tumors that had developed from metastasizing cells. As candidates for metastasis-related genes that were targets of the isolated ribozymes, we identified five unknown and three known genes: stromal interaction molecule 1 (*STIM1*), polymerase γ2 accessory subunit (*Polg2*), and cytochrome P450, family 2, subfamily d, polypeptide 22 (*Cyp2d22*). Repression of four of these by small interfering RNAs indeed resulted in the accelerated mobility of cells in *in vitro* scratch-wound assay. The further characterization of these candidate genes would provide clues to the complex mechanism(s) of metastasis.

Hammerhead ribozymes (referred to herein after as ribozymes) that specifically cleave the transcripts of particular genes can be produced when the nucleotide sequences of the substrate-recognition arms are designed such that they are complementary to the sequences of individual target mRNAs. Such ribozymes have been used successfully to interfere with the expression of specific genes via cleavage of the respective target mRNAs in mammalian cells (1–6). The use of a library of ribozymes with randomized substrate-recognition arms allowed the identification of genes that are involved directly in certain phenomena, such as the transformation of NIH3T3 fibroblasts, anchorage-independent cell growth, tumor necrosis factor-α-induced apoptosis and tumor invasion (7–15).

The metastatic spread of tumor cells around the body is a key target for cancer therapy (16, 17). An experimental assay of metastasis *in vivo* that involves intravenous injection of tumor cells into mice was developed by Fidler (18) for the analysis of the metastatic properties of melanoma cells (Fig. 1). In this assay, cells of interest are injected into the tail vein of mice and allowed to proliferate and/or metastasize. After several weeks, pulmonary metastases are observed in the case of strongly metastatic melanoma cells, while relatively few metastases are formed after injection of cells with limited metastatic potential. This assay allows the selection of strongly metastatic cells from a heterogeneous population of weakly metastatic tumor cells (18, 19). Thus, the assay allows not only the study of the metastatic characteristics of melanoma cells but also the isolation of strongly metastatic cells. In the present study, we used this mouse model and mouse B16F0 melanoma cells, a weakly metastatic melanoma cell line, to investigate the applicability of a library of ribozymes *in vivo*, to isolate ribozymes that converted weakly metastatic melanoma cells to strongly metastatic cells by the apparent disruption of expression of specific gene(s), and to identify genes related to metastasis.

EXPERIMENTAL PROCEDURES

Construction of a Ribozyme Library—A library of ribozymes was constructed based on the retrovirus expression vector pMXpuro (20). First, fragments of DNA carrying randomized hammerhead ribozymes were obtained by PCR amplification using oligonucleotide DNAs as follows, a sense primer (5′-TCC CCG GTT CGA AAC CGG GCA-3′), an antisense primer (5′-GCT TGC ATG CCT GCA GGT CGA CGC GAT AGA AAA AAA GAT ATC CGG GGT-3′), and a template (5′-TCC CCG GTT CGA AAC CGG GCA CTA CAA AAA CCA ACT TTN NNN NNNN CTG ATG AGG CCG AAA GGC CGA AAN NNN NNNG GTA CCC CGG ATA TCT TTT TTT-3′, where N represents A, T, G, or C). The fragments were cloned into a plasmid vector, pGEM-T (Promega, Madison, WI), then were digested with Csp45I and KpnI, and were again cloned into pPUR-KE (21). Next, fragments encoding $tRNA^{Val}$-fused randomized ribozymes were obtained by digestion of the library of ribozymes based on pPUR-KE with EcoRI and BamHI. Finally, the fragments were inserted into the EcoRI and BamHI sites in pMXpuro.

Cell Culture and Retroviral Infection—B16F0 melanoma cells (number CRL-6322; ATCC, Manassas, VA) were cultured in Dulbecco's modified Eagle's medium (Sigma) supplemented with 10% fetal bovine serum (Invitrogen) and an antibiotics mixture (Invitrogen). Retroviral preparation and infection with the retroviral vector pMXpuro and the packaging cell line Plat-E (kindly provided by Professor Toshio Kitamura, Institute of Medical Science, University of Tokyo, Tokyo, Japan) were performed as described elsewhere (14, 20). Infected cells were treated with medium that contained puromycin (1 μg/ml, Sigma) for 4 weeks.

Experimental Metastasis Assay—5×10^6 of B16F0 cells, infected with retroviruses carrying a ribozyme library or not, were suspended in phosphate-buffered saline (PBS[1]; Takara Bio, Shiga, Japan) and intravenously injected into the lateral tail vein of C57BL/6NCrj mice (Charles River Japan, Yokohama, Japan). Two weeks after injection, lungs were removed from the mice and were washed with ice-cold PBS. The pulmonary metastases on the surface of the lungs were observed and counted. Then the nodules were removed, minced, and cultured in dishes.

RT-PCR Analysis and Ribozyme Rescue—Total RNA was prepared from cells using the Isogen reagent (Nippon Gene, Toyama, Japan) according to the manufacturer's protocol. cDNA was synthesized using

* The costs of publication of this article were defrayed in part by the payment of page charges. This article must therefore be hereby marked "*advertisement*" in accordance with 18 U.S.C. Section 1734 solely to indicate this fact.

¶ These authors contributed equally to this work.

‖ To whom correspondence should be addressed: Dept. of Chemistry and Biotechnology, School of Engineering, The University of Tokyo, 7-3-1 Hongo, Bunkyo-ku, Tokyo 113-8656, Japan. Tel.: 81-3-5841-8828; Fax: 81-3-5841-8828; E-mail: taira@chembio.t.u-tokyo.ac.jp.

[1] The abbreviations used are: PBS, phosphate-buffered saline; RT, reverse transcriptase; siRNA, small interfering RNA; *STIM1*, stromal interaction molecule 1 gene; *Polg2*, polymerase γ2 accessory subunit gene; *Cyp2d22*, cytochrome P450, family 2, subfamily d, polypeptide 22 gene.

2 μg of total RNA and Moloney murine leukemia virus reverse transcriptase (Promega). Using the cDNA as templates, PCR amplification was performed with primers as follows: ribozyme sense, 5′-TCC CCG GTT CGA AAC CGG GCA-3′; ribozyme antisense, 5′-GCT TGC ATG CCT GCA GGT CGA CGC GAT AGA AAA AAA GAT ATC CGG GGT-3′; β-actin sense, 5′-GCA CGG CAT CGT CAC CAA CT-3′; and β-actin antisense, 5′-AAG GCT GGA AGA GTG CCT CA-3′. The amplified fragments of DNA were confirmed by agarose gel electrophoresis. Fragments carrying ribozymes that were derived from the metastatic nodules were cloned into the pGEM-T vector (Promega) and sequenced.

Search of DNA Data Bases—By searching of mouse cDNA databases with the BLAST program, identification of target genes of the selected ribozymes was performed (22) (www3.ncbi.nlm.nih.gov/BLAST/). Parameters for the data base searches were set to optimize searches for short, nearly exact sequences.

Construction and Transfection of siRNA Expression Plasmid—Plasmid vectors encoding siRNAs for four of the eight identified targets were constructed as described (23). Two target sites for each of the genes were selected using an algorithm (www.igene-therapeutics.co.jp). Transfections were performed using LipofectAMINE Plus (Invitrogen). Typically, 3 μg of plasmid DNA was used per 80% confluent 6-cm dish culture. Transfected B16F0 cells were selected in medium containing puromycin (2.5 μg/ml) for 48 h and then subjected to RT-PCR analysis and *in vitro* scratch-wound assay. The expression of targeted genes was examined by gene-specific primers, *STIM1* (sense: 5′-GGG AAG ACC TCA ATT ACC A-3′ and antisense: 5′-CAG CTG CAG CTT CTG CCT GT-3′), *Polg-2* (sense: 5′-GGG AAG CAA ACT TTA CTA CAA CT-3′ and antisense: 5′-ATC CAA AGC GAC CTT AAT AG-3′), and *Cyp2d22* (sense: 5′-AAG GAG GAA GCT GGA TTC CTA CC-3′ and antisense: 5′-CCC TAT GAC TTC ATC GAT TT-3′), on standard condition for RT-PCR (25 cycles of 94 °C for 30 s, −54 °C for 60 s, −72 °C for 60 s).

Scratch-wound Assay—B16F0 cells that had been treated with siRNA expression plasmid were allowed to form a monolayer on a fibronectin (10 μg/ml)-coated dish surface. A wound was made in the monolayer of cells by completely scratching the cells in a line with a pipette tip. Cells were washed a few times with PBS to remove cell debris and fed with fresh medium as described (14). The time of the scratching wound was designated as time 0. Cells were allowed to proliferate and migrate into the wound during the next 30 h. Migration of cells into the wound was recorded under a phase contrast microscope with a 10× phase objective.

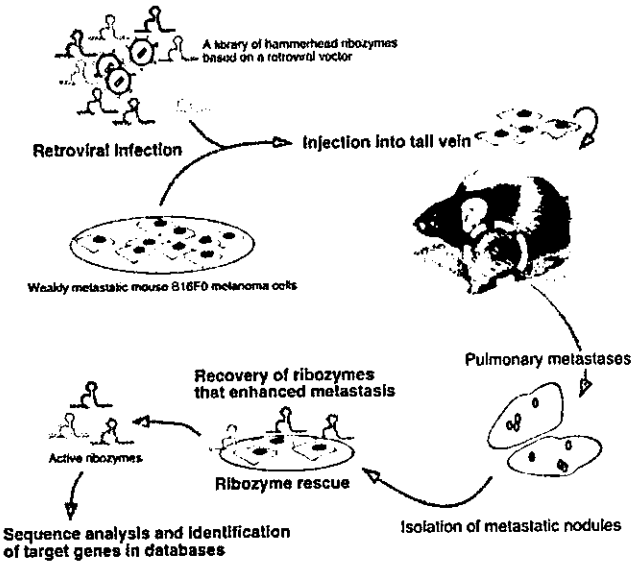

FIG. 1. **Strategy for the identification of genes using a randomized library of hammerhead ribozymes and the assay *in vivo* for the determination of the metastatic potential of melanoma cells.**

RESULTS AND DISCUSSION

We constructed a library of ribozymes that was based on the retroviral expression vector pMXpuro (20). Retroviruses carrying randomized ribozymes were prepared in the packaging cell line Plat-E as described elsewhere (14, 20). Then we infected weakly metastatic B16F0 cells with the retroviruses for the selection of ribozymes that enhanced the metastatic properties

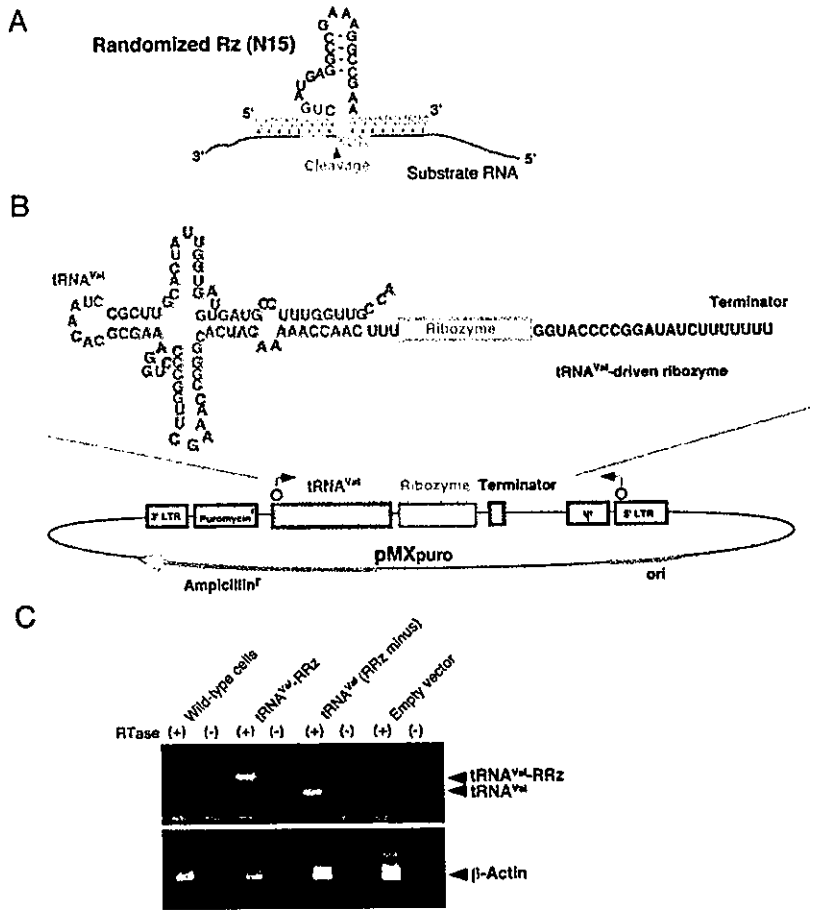

FIG. 2. **The randomized ribozyme.** *A*, *red letters* indicate the randomized recognition arms of the hammerhead ribozyme (*Rz*). Substrate RNAs contain a NUX triplet (where N and *X* represent A, U, G, or C and A, U, or C, respectively) that is susceptible to cleavage by hammerhead ribozymes (3). *B*, the structure of the retroviral vector, pMXpuro, that carried the randomized ribozymes. Ribozymes were expressed as $tRNA^{Val}$-fused RNAs. *LTR*, long terminal repeat. *C*, cells were infected with retroviruses that carried a $tRNA^{Val}$-fused randomized ribozyme (*RRz*) or $tRNA^{Val}$ alone (*RRz minus*) or with the empty vector (*$tRNA^{Val}$* and *RRz minus*). The expression of $tRNA^{Val}$-fused RRz or $tRNA^{Val}$ (*RRz minus*) was confirmed by RT-PCR analysis. Results of RT-PCR for β-actin mRNA are also shown as internal controls. Symbols (+) and (−) refer to assays with and without reverse transcriptase (*RTase*). Cells infected with the retrovirus that carried $tRNA^{Val}$ alone (*RRz minus*) were used as controls in subsequent experiments.

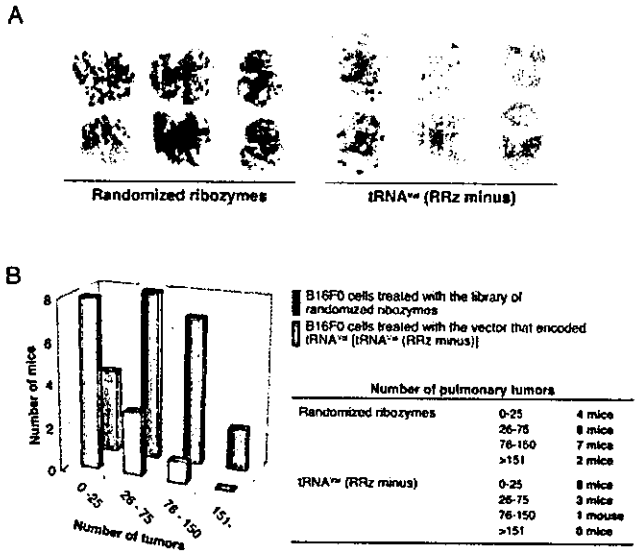

FIG. 3. **Selection *in vivo* of ribozymes that enhanced the metastatic properties of B16F0 melanoma cells, using a mouse model and cells treated with the library of randomized ribozymes.** *A*, isolation of pulmonary metastases. *B*, number of pulmonary tumors isolated after the injection of B16F0 cells that had been treated with randomized ribozymes (*RRz*) or tRNA^{Val} alone (*RRz minus*).

TABLE I
Selected ribozymes and their target genes

Selected ribozymes and their target genes

	Recognition arm		Recognition arm
RRzA:	ATCGATCG		AGTCTCCC
RRzB:	CTCCGTTG		ATTCGATT
RRzC:	CTTTCGCG		ATACGAAC
RRzD:	GCGCGGAG		ACAGGTAT
RRzE:	GCTTACTC		ACGTGAGG
RRzF:	GCATGGGC		ATCCCCAT
RRzG:	GTGACCGC		ACGTGTCG
RRzH:	GTCGACCA		ATTGTAGG

Target sequence	Target gene
RRzA: GGGAGACTNCGATCGAT	*Mus musculus* stromal interaction molecule 1, (cDNA clone MGC:13964 IMAGE:4191156) GenBank accession number: BC021644.1
RRzB: AATCCAATNCAACGCAG	*Mus musculus* expressed sequence AW551984 (AW551984) GenBank accession number: NM_178737.1
RRzC: GTTCGTATNCGCGAAAG	*Mus musculus* polymerase (DNA-directed), gamma 2, accessory subunit (Polg2) GenBank accession number: NM_015810.1
RRzD: ATACCTGTNCTCCGCGC	*Mus musculus* cytochrome P450, family 2, subfamily d, polypeptide 22 (Cyp2d22) GenBank accession number: NM_019823.1
RRzE: CCTCACGTNGGGGAAGC	*Mus musculus* LOC230840 (LOC230840) GenBank accession number: XM_161442.1
RRzF: ATGGGGATNGCCCATCC	*Mus musculus* hypothetical gene; supported by AK030301 (LOC328981) GenBank accession number: XM_286862.1
RRzG: CCACACGTNGCGGGTAC	Unidentified
RRzH: CCTACAATNTGGTCGAC	*Mus musculus* hypothetical gene; supported by AK040634 (LOC329840) GenBank accession number: XM_287326.1

of the cells (Fig. 2, *A* and *B*). After antibiotic (puromycin) selection, we confirmed the expression of randomized ribozymes in cells by RT-PCR analysis with primers specific for the parent ribozyme (Fig. 2*C*). Then we injected 5×10^5 control or randomized ribozymes harboring B16F0 cells intravenously into the lateral tail vein of individual C57BL/6N mice. Cells with enhanced metastatic properties were selected by their isolation from lung as pulmonary tumors. Only a few pulmonary metastases were detected in the mice injected with parent B16F0 cells as reported earlier (18, 19). Fig. 3, *A* and *B*, show the difference in terms of the resultant pulmonary metastases

TABLE II
siRNA target sequence

Gene	Target site	Sequence
STIM1	Site 1	GGGAAGACCTCAATTACCA
	Site 2	GGCCAAGAAGACATTTATA
AW551984	Site 1	GAACAAACTTCTATCTTTA
	Site 2	AGTCAAACTTGTAAATAGA
Polg2	Site 1	GAAGCAAACTTTACTACAA
	Site 2	GGGAAAGGAGCCAATAGAA
Cyp2d22	Site 1	GAAGGAAACTCTTAAGGAA
	Site 2	GCGCCGAGTACAACAGGAA

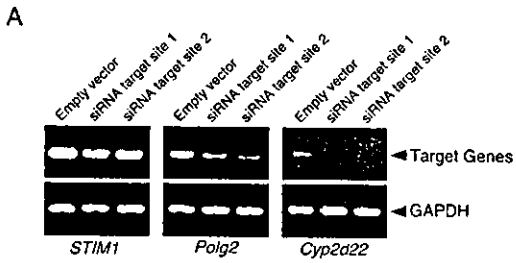

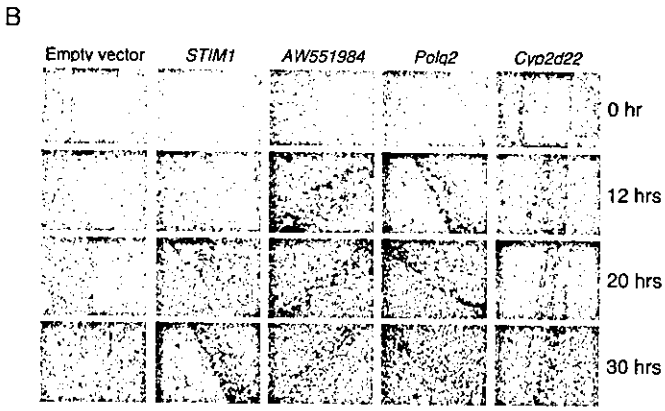

FIG. 4. **Silencing of *STIM1*, *AW551984*, *Polg2*, and *Cyp2d22* by siRNA expression vector.** *A*, expression levels of target genes were confirmed by RT-PCR analysis. Results of RT-PCR for glyceraldehyde-3-phosphate dehydrogenase (*GAPDH*) mRNA are also shown as internal controls. *B*, scratch-wound assay. Movement of cells into the wound is shown for cells transfected with empty vector (control) or siRNA expression vectors (target site 2) against *STIM1*, *AW551984*, *Polg2*, and *Cyp2d22*.

between cells that had been treated with the ribozyme library and untreated cells, 2 weeks after injection. The number of metastatic melanoma nodules derived from library-treated cells was clearly higher than those derived from untreated cells. Thus, certain ribozymes in the library appeared to have promoted the pulmonary metastasis of B16F0 cells (Fig. 3, *A* and *B*).

Next, we removed the pulmonary nodules of melanoma cells derived from ribozyme harboring cells (Fig. 3*A*), and we collected cells from these nodules by mincing and treating them with trypsin. The resultant cells were cultured, and RNA was isolated from these cells. Then ribozymes were amplified by RT-PCR strategy and cloned into plasmid vector (15) (Fig. 1), and the results of sequencing of the ribozymes indicated that the selected ribozymes represented eight types of ribozyme that contained specific substrate-recognition arms (Table I). By this way, we recovered ribozymes that appeared to have raised the metastatic potential of B16F0 cells.

We then identified their target genes by searching data bases with the BLAST program, using settings that optimized searches for short, nearly exactly matching sequences (22) (www3.ncbi.nlm.nih.gov/BLAST/) (Table I). Among the selected ribozymes, our search indicated that ribozyme A targeted the transcript of the gene known as stromal interaction molecule 1 (*STIM1*). *STIM1* is a gene for a transmembrane glycoprotein. This gene is located at human chromosome region 11p15.5, which is involved in tumorigenesis. Moreover, overexpression of *STIM1* causes growth arrest and cell death in several lines of cells (24, 25). These earlier observations indicate that *STIM1* functions as a tumor suppressor. Therefore, our identification of a ribozyme that targets *STIM1* in our assay of metastasis by cells treated with a ribozyme library seems eminently reasonable. Our data base search also identified genes whose functions have not yet been well characterized, such as the sequence AW551984, expressed in the mouse, which contains a VWA domain that seems to mediate adhesion of eukaryotic cells (a target for ribozyme B; GenBank™ accession number NM_178737.1; Table I).

We next constructed siRNA expression vectors against four (*STIM1*, *AW551984*, *Polg2*, and *Cyp2d22*) out of the eight identified genes and examined their functional involvement in metastasis by carrying out a scratch-wound assay that is commonly used to study the ability of cells to migrate (26, 27), a reliable parameter for metastasis. We prepared two different siRNA expression vectors for each of target genes (Table II). Cells harboring the expression plasmid were selected in puromycin supplemented medium. We examined suppression of the expression of target genes and confirmed reduced levels of expression of three genes, *STIM1*, *Polg2*, and *Cyp2d22* (unfortunately, *AW551984* transcript could not be detected by RT-PCR analysis) (Fig. 4*A*). Then we subjected the cells to the scratch-wound assay (Fig. 4*B*). Targeting of all the four genes led to significant acceleration of migration, which is one of the properties of metastatic cells. *AW551984*- and *Polg2*-targeted B16F0 cells moved more than 90% of the width of the wound in 30 h, whereas control cells, which had been treated with empty vector, only initiated to migrate into the wound. Parallel observation on *STIM1*- and *Cyp2d22*-targeted cells revealed about 50% movement into the wound (Fig. 4*B*). Although siRNA-induced suppression of *AW551984* could not be confirmed due to technical difficulty in RT-PCR analysis, the change in phenotype (increased migration) was obtained in two independent experiments. Taken together, these four genes appeared to have a role in control of the metastatic properties of B16F0 melanoma cells. Further investigation of genes identified in this study would provide important clues to the complex mechanism(s) of metastasis.

To the best of our knowledge, this is the first demonstration of the applicability of a ribozyme library to the identification of genes using animal model. To date, such a potential has been demonstrated only in cultured cells (7–15, 28, 29). It should now be possible to identify important functional genes *in vivo* using randomized ribozyme libraries.

Acknowledgments—We thank Dr. Toshio Kitamura (Institute of Medical Science, University of Tokyo) for supplying the retroviral vector pMXpuro and the packaging cell line Plat-E, as well as Drs. Motowo Nakajima and Tatsuhiko Kasaoka (Tsukuba Research Institute, Novartis Pharma, Tsukuba Science City) for critical comments and helpful discussions.

REFERENCES

1. Uhlenbeck, O. C. (1987) *Nature* **328,** 596–600
2. Haseloff, J., and Gerlach, W. L. (1988) *Nature* **334,** 585–591
3. Zhou, D. M., and Taira, K. (1998) *Chem. Rev.* **98,** 991–1026
4. Kawasaki, H., Eckner, R., Yao, T. P., Taira, K., Chiu, R., Livingston, D. M., and Yokoyama, K. K. (1998) *Nature* **393,** 284–289
5. Gasteland, R. F., Cech, T. R., and Atkins, J. F. (1999) *The RNA World*, 2nd Ed., Cold Spring Harbor Laboratory Press, Cold Spring Harbor, NY
6. Krupp, G., and Gaur, R. K. (2000) *RIBOZYME: Biochemistry and Biotechnology*, Eaton Publishing, Natick, MA
7. Kruger, M., Beger, C., Li, Q. X., Welch, P. J., Tritz, R., Leavitt, M., Barber, J. R., and Wong-Staal, F. (2000) *Proc. Natl. Acad. Sci. U. S. A.* **97,** 8566–8571
8. Li, Q. X., Robbins, J. M., Welch, P. J., Wong-Staal, F., and Barber, J. R. (2000) *Nucleic Acids Res.* **28,** 2605–2612
9. Welch, P. J., Marcusson, E. G., Li, Q. X., Beger, C., Kruger, M., Zhou, C., Leavitt, M., Wong-Staal, F., and Barber, J. R. (2000) *Genomics* **66,** 274–283
10. Beger, C., Pierce, L. N., Kruger, M., Marcusson, E. G., Robbins, J. M., Welcsh, P., Welch, P. J., Welte, K., King, M. C., Barber, J. R., and Wong-Staal, F. (2001) *Proc. Natl. Acad. Sci. U. S. A.* **98,** 130–135
11. Kawasaki, H., Onuki, R., Suyama, E., and Taira, K. (2002) *Nat. Biotechnol.* **4,** 376–380
12. Kawasaki, H., and Taira, K. (2002) *EMBO Rep.* **3,** 443–450
13. Suyama, E., Kawasaki, H., Kasaoka, T., and Taira, K. (2003a) *Cancer Res.* **63,** 119–124
14. Suyama, E., Kawasaki, H., Nakajima, M., and Taira, K. (2003b) *Proc. Natl. Acad. Sci. U. S. A.* **100,** 5616–5621
15. Nelson, L. D., Suyama, E., Kawasaki, H., and Taira, K. (2003) *Targets* **2,** 191–200
16. Tannock, I. F., and Hill, R. P. (1998) *The Basic Science of Oncology*, 3rd Ed., The McGraw-Hill Companies, New York
17. Holland, J. F., and Frei, E. (2000) *Cancer Medicine*, 5th Ed., B. C. Decker, Hamilton, Canada
18. Fidler, I. J. (1973) *Nat. New Biol.* **242,** 148–149
19. Clark, E. A., Golub, T. R., Lander, E. S., and Hynes, R. O. (2000) *Nature* **406,** 532–535
20. Morita, S., Kojima, T., and Kitamura, T. (2000) *Gene Ther.* **7,** 1063–1066
21. Koseki, S., Tanabe, T., Tani, K., Asano, S., Shioda, T., Nagai, Y., Shimada, T., Ohkawa, J., and Taira, K. (1999) *J. Virol.* **73,** 1868–1877
22. Altschul, S. F., Madden, T. L., Schaffer, A. A., Zhang, J., Zhang, Z., Miller, W., and Lipman, D. J. (1997) *Nucleic Acids Res.* **25,** 3389–3402
23. Wadhwa, R., Kaul, S. C., Miyagishi, M., and Taira, K. (2004) *Rev. Mutat. Res.*, in press
24. Sabbioni, S., Barbanti-Brodano, G., Croce, C. M., and Negrini, M. (1997) *Cancer Res.* **57,** 4493–4497
25. Manji, S. S., Parker, N. J., Williams, R. T., van Stekelenburg, L., Pearson, R. B., Dziadek, M., and Smith, P. J. (2000) *Biochim. Biophys. Acta* **1481,** 147–155
26. Magdalena, J., Millard, T. H., and Machesky, L. M. (2003) *J. Cell Sci.* **116,** 743–756
27. Ettenson, D. S., and Gotileb, A. I. (1995) *Arterioscler. Thromb. Vasc. Biol.* **15,** 515–521
28. Onuki, R., Bando, Y., Suyama, E., Katayama, T., Kawasaki, H., Baba, T., Tohyama, M., and Taira, K. (2004) *EMBO J.* **23,** 959–968
29. Kuwabara, T., Hsieh, J., Nakashima, K., Taira, K., and Gage, F. H. (2004) *Cell* **116,** 779–793

J|A|C|S
ARTICLES
Published on Web 11/09/2004

NMR-Based Reappraisal of the Coordination of a Metal Ion at the Pro-*Rp* Oxygen of the A9/G10.1 Site in a Hammerhead Ribozyme

Ken-ichi Suzumura,[†] Yasuomi Takagi,[‡] Masaya Orita,[†] and Kazunari Taira*[,§,∥]

Contribution from the Yamanouchi Pharmaceutical Co., Ltd., 21 Miyukigaoka, Tsukuba Science City, 305-8585, Japan, iGENE Therapeutics Inc., Central 4, 1-1-1 Higashi, Tsukuba Science City, 305-8562, Japan, Gene Function Research Center, National Institute of Advanced Industrial Science and Technology (AIST), Tsukuba Central 4, 1-1-1 Higashi, Tsukuba Science City, 305-8562, Japan, and Department of Chemistry and Biotechnology, School of Engineering, The University of Tokyo, 7-3-1 Hongo, Tokyo 113-8656, Japan

Received May 9, 2004; E-mail: taira@chembio.t.u-tokyo.ac.jp

Abstract: In the identification of a metal-binding site within enzymes, kinetic analyses based on thio-effects and Cd^{2+}-rescues are widely used. In those analyses, kinetic studies using a phosphorothioate have been discussed on the premise that the substitution by a sulfur atom does not change the conformation of a ribozyme. However, our present NMR structural analysis demonstrates the change of the conformation at the metal-binding site by ***Rp***-sulfur but not by ***Sp***-sulfur substitution and warns against incautious interpretations of thio-effects and rescue phenomena in kinetic studies using a phosphorothioate. Our analysis further demonstrates that, in solution, a Cd^{2+} ion can interact with an ***Rp***-phosphorothioate (in support of the controversial McKay's structure, *Nature* **1994**, *372*, 68−74) and with an ***Sp***-phosphorothioate (in support of the controversial Scott's structure, *Cell* **1995**, *81*, 991−1002) at the metal-binding A9/G10.1 site and that, in the former case, the bound Cd^{2+} ion can return the ribozyme to an active conformation and rescue its enzymatic activity.

The hammerhead ribozyme is a self-cleaving RNA that is found in small RNA plant pathogens, and it catalyzes the sequence-specific cleavage of RNA. Metal ions play an important role in the catalytic cleavage of the phosphodiester bond in an RNA by hammerhead ribozymes and the reaction yields a 2′,3′-cyclic phosphate.[1] Studies by X-ray crystallography have facilitated analysis of the mechanism of action of these ribozymes.[2] The crystal structure obtained by McKay's group revealed a metal-binding site, A9/G10.1, located in the vicinity of domain II, which forms a continuous stack between stem II and stem III.[2a] In this crystal structure, an Mn^{2+} ion binds between the pro-***Rp*** oxygen of the phosphate group of A9 (P9 oxygen) and the N7 atom of G10.1. Even though this metal-binding site (A9/G10.1 site) within the crystal structure is located approximately 20 Å from the scissile phosphodiester bond, this metal-binding site is thought to play a crucial role in achieving maximal cleavage activity for the following reasons. Replacement of the pro-***Rp***-phosphoryl P9 oxygen atom by a sulfur atom results in a dramatic decrease in Mg^{2+}-dependent catalytic activity.[3] Furthermore, replacement of G10.1 by a pyrimidine also results in a substantial decrease in the ribozyme's activity.[4] Moreover, the addition of a low concentration of Cd^{2+} ions, which are thiophilic, to a solution of the ribozyme with an ***Rp***-phosphorothioate linkage returns the rate of the catalytic reaction to the control value.[5]

[†] Yamanouchi Pharmaceutical Co., Ltd.
[‡] iGENE Therapeutics Inc.
[§] Gene Function Research Center, National Institute of Advanced Industrial Science and Technology.
[∥] Department of Chemistry and Biotechnology, School of Engineering, The University of Tokyo.

(1) (a) Lilley, D. M. J. *Curr. Opin. Struct. Biol.* **1999**, *9*, 330−338. (b) Scott, E. C.; Uhlenbeck, O. C. *Nucleic Acids Res.* **1999**, *27*, 479−484. (c) Wang, S.; Karbstein, K.; Peracchi, A.; Beigelman, L.; Herschlag, D. *Biochemistry* **1999**, *38*, 14363−14378. (d) Murray, J. B.; Scott, W. G. *J. Mol. Biol.* **2000**, *296*, 33−41. (e) Nakamatsu, Y.; Kuwabara, T.; Warashina, M.; Tanaka, Y.; Yoshinari, K.; Taira, K. *Genes Cells* **2000**, *5*, 603−612. (f) O'Rear, J. L.; Wang, S.; Feig, A. L.; Beigelman, L.; Uhlenbeck, O. C.; Herschlag, D. *RNA* **2001**, *7*, 537−545. (g) Curtis, E. A.; Bartel, D. P. *RNA* **2001**, *7*, 546−552. (h) Takagi, Y.; Warashina, M.; Stec, W. J.; Yoshinari, K.; Taira, K. *Nucleic Acids Res.* **2001**, *29*, 1815−1834. (i) Hammann, C.; Norman, D. G.; Lilley, D. M. J. *Proc. Natl. Acad. Sci. U.S.A.* **2001**, *98*, 5503−5508 (j) Burke, J. M. *Biochem. Soc. Trans.* **2002**, *30*, 1115−1118. (k) Hammann, C.; Lilley, D. M. J. *ChemBioChem* **2002**, *3*, 690−700. (l) Zhou, J. M.; Zhou, D. M.; Takagi, Y.; Kasai, Y.; Inoue, A.; Baba, T.; Taira, K. *Nucleic Acids Res.* **2002**, *30*, 2374−2382. (m) Inoue, A.; Takagi, Y.; Taira, K. *Magnes. Res.* **2003**, *16*, 210−217. (n) Takagi, Y.; Ikeda, Y.; Taira, K. *Topics Curr. Chem.* **2004**, *232*, 213−251. (o) Warashina, M.; Kuwabara, T.; Nakamatsu, Y.; Takagi, Y.; Kato, Y.; Taira, K. *J. Am. Chem. Soc.* **2004**, *126*, 12291−12297. (p) Takagi, Y.; Inoue, A.; Taira, K. *J. Am. Chem. Soc.* **2004**, *126*, 12856−12864.

(2) (a) Pley, H. W.; Flaherty, K. M.; McKay, D. B. *Nature* **1994**, *372*, 68−74. (b) Scott, W. G.; Finch, J. T.; Klug, A. *Cell* **1995**, *81*, 991−1002. (c) Scott, W. G.; Murray, J. B.; Arnold, J. R. P.; Stoddard, B. L.; Klug, A. *Science* **1996**, *274*, 2065−2069. (d) Murray, J. B.; Terwey, D. P.; Maloney, L.; Karpeisky, A.; Usman, N.; Beigelman, L.; Scott, W. G. *Cell* **1998**, *92*, 665−673. (e) Murray, J. B.; Szöke, H.; Szöke, A.; Scott, W. G. *Mol. Cell* **2000**, *5*, 279−287. (f) Scott, W. G. *J. Mol. Biol.* **2001**, *311*, 989−999. (g) Murray, J. B.; Dunham, C. M.; Scott, W. G. *J. Mol. Biol.* **2002**, *315*, 121−130.

(3) Ruffner, D. E.; Uhlenbeck, O. C.; *Nucleic Acids Res.* **1990**, *18*, 6025−6029.

(4) (a) Ruffner, D. E.; Stormo, G. D.; Uhlenbeck, O. C. *Biochemistry* **1990**, *29*, 10695−10702. (b) Tuschl, T.; Eckstein, F. *Proc. Natl. Acad. Sci. U.S.A.* **1993**, *90*, 6991−6994.

(5) Peracchi, A.; Beigelman, L.; Scott, E. C.; Uhlenbeck, O. C.; Herschlag, D. *J. Biol. Chem.* **1997**, *272*, 26822−26826.

10.1021/ja0472937 CCC: $27.50

The results of crystallographic and kinetic studies have indicated that binding of a metal ion at the pro-***Rp*** oxygen of A9/G10.1 site is of critical importance for enzymatic catalysis by hammerhead ribozymes.[2a,5] However, this conclusion remains controversial. For example, in the crystal structure obtained by Scott's group, the metal ion does not bind at the pro-***Rp*** oxygen but, instead, it binds at the pro-***Sp*** oxygen. To be specific, $Mg(H_2O)_5^{2+}$ binds directly to the pro-***Sp*** oxygen of A9 and is associated, via the hydration shell, with the exocyclic oxygen O6 of G8, with N7 of G10.1, and with N2 of G12.[2b] This potential $Mg(H_2O)_5^{2+}$-binding site corresponds to the Mn^{2+}-binding site identified by McKay's group in their crystal structure of a hammerhead ribozyme. Furthermore, ^{31}P NMR studies using phosphorothioates indicated that a metal ion binds to both the pro-***Sp*** and pro-***Rp*** oxygen. The ^{31}P NMR signals from ***Rp***- and ***Sp***-phosphorothioates at A9 in hammerhead ribozymes moved 2−3 ppm upfield shift upon the addition of one to two molar equivalents of Cd^{2+} ions.[6] Finally, in studies of the metal-binding motifs GA10***Sp***S and GA10***Rp***S, we found that binding of a metal ion was supported at both the pro-***Sp*** and the pro-***Rp*** position.[7]

The oligomers designated GA10***Sp***S and GA10***Rp***S are derivatives of the well-characterized GA10 oligomer,[8] whose sequence is shown in Figure 1, and they have a phosphorothioate group at A6, which corresponds to the A9 metal-binding site of a hammerhead ribozyme. Even though GA10 corresponds to the structure of only part of a hammerhead ribozyme-substrate complex (R32−S11; Figure 1), GA10 is analogous to the A9/G10.1 motif of the hammerhead ribozyme since GA10 includes a sheared-type tandem G12-A9 pair as a metal-binding site in the duplex, and it has been demonstrated that the GA10 molecule is sufficient to allow capture of divalent cations in the absence of any of the other conserved residues that are found in hammerhead ribozymes.[8b,c,d]

In our previous study, to clarify the functions of the pro-***Rp*** and the pro-***Sp*** positions at the cleavage site and the A9/G10.1 metal-binding site of the hammerhead ribozyme, we employed GA10***Sp***S and GA10***Rp***S as metal-binding motifs at the A9/G10.1 site.[7] The ^{31}P signals from both the ***Rp***- and the ***Sp***-phosphorothioate of GA10***Sp***S and of GA10***Rp***S moved considerably upfield upon the addition of Cd^{2+} ions to solutions of GA10***Rp***S and GA10***Sp***S. At 9 molar equiv of Cd^{2+} ions, the extent of perturbations of the phosphorothioate signals were close to the maximum, indicating saturation by Cd^{2+} ions of both GA10***Rp***S and GA10***Sp***S. At saturation (9 molar equiv Cd^{2+} ions), the chemical shifts were 10 and 6 ppm higher than those of GA10***Rp***S and GA10***Sp***S, respectively, in the absence of Cd^{2+} ions. Our previous studies with GA10***Sp***S and GA10***Rp***S also demonstrated that a Cd^{2+} ion is able to bind to both the ***Sp*** and the ***Rp*** sulfur atom in the absence of domain I (catalytic domain, formation by C3, U4, G5, A6, and C17 in Figure 1) of the hammerhead ribozyme. However, the nature and the conformation of the metal-binding sites in the presence of ***Rp***- and ***Sp***-phosphorothioates and in the absence of bound metal ions remain to be investigated. The exact effects of metal ions at the catalytically significant P9 site and their roles in the catalytic activity of hammerhead ribozymes remain to be clarified.

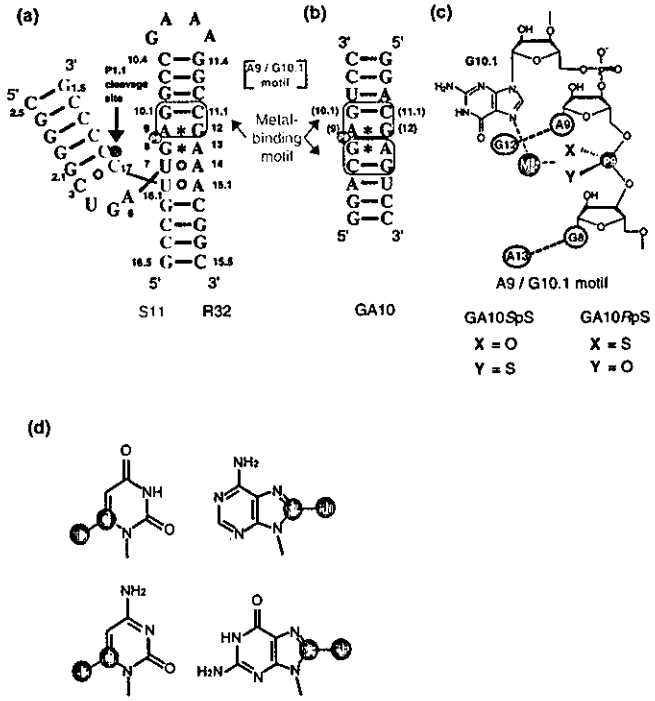

Figure 1. Sequences and secondary structures of (a) a hammerhead ribozyme (R32) and its substrate (S11). The black arrow indicates the cleavage site. (b) Sequence and secondary structure of GA10. The metal-binding motifs (the A9/G10.1 motif of the hammerhead ribozyme) are surrounded by magenta lines. In panels (a) and (b), Watson−Crick base pairs, non-Watson−Crick base pairs, and sheared-type G:A pairs are indicated by bars, open circles, and asterisks, respectively. GA10***Sp***S and GA10***Rp***S each have a phosphorothioate moiety at the A6 position, which corresponds to the A9 position of the hammerhead ribozyme. (c) Schematic representation of the A9/G10.1 motif. (d) Atoms in nucleobases that were monitored in natural-abundance $^1H-^{13}C$ HSQC.

Previous NMR investigations on the effects of a phosphorothioate on RNA structure led to two different conclusions.[9] One group observed a conformational change within an RNA hairpin by the introduction of an ***Rp***-phosphorothioate at the binding site of the phage MS2 capsid protein.[9a] The other group did not observe any structural changes by an ***Sp***-phosphorothioate modification at the metal binding site of yeast U6 RNA.[9b] The corresponding detailed structural study has not been performed for the hammerhead ribozyme with a phosphorothioate at the metal binding site, although limited ^{31}P NMR studies were reported.[6,7] In the present analysis, to elucidate the mechanism of binding of metal ions in the vicinity of the phosphate group at A9/G10.1, we examined the physicochemical properties of GA10***Sp***S and GA10***Rp***S by ^1H NMR, ^{31}P NMR, and ^1H-^{13}C HSQC spectroscopy. The ^1H, ^{13}C, and ^{31}P NMR signals of GA10***Sp***S in the absence and in the presence of Cd^{2+} ions were, respectively, similar to those of the unmodified parental RNA,

(6) Maderia, M.; Hunsicker, L. M.; DeRose, V. J. *Biochemistry* **2000**, *40*, 12113−12120.
(7) Suzumura, K.; Yoshinari, K.; Tanaka, Y.; Takagi, Y.; Kasai, Y.; Warashina, M.; Kuwabara, T.; Orita, M.; Taira, K. *J. Am. Chem. Soc.* **2002**, *124*, 8230−8236.
(8) (a) Katahira, M.; Kanagawa, M.; Sato, H.; Uesugi, S.; Fujii, S.; Kohno, T.; Maeda, T. *Nucleic Acids Res.* **1994**, *22*, 2752−2759. (b) Tanaka, Y.; Morita, E. H.; Hayashi, H.; Kasai, Y.; Tanaka, T.; Taira, K. *J. Am. Chem. Soc.* **2000**, *122*, 11303−11310. (c) Tanaka, Y.; Kojima, C.; Morita, E. H.; Kasai, Y.; Yamasaki, K.; Ono, A.; Kainosho, M.; Taira, K. *J. Am. Chem. Soc.* **2002**, *124*, 4595−4601. (d) Tanaka, Y.; Kasai, Y.; Mochizuki, S.; Wakisaka, A.; Morita, E. H.; Kojima, C.; Toyozawa, A.; Kondo, Y.; Taki, M.; Takagi, Y.; Inoue, A.; Yamasaki, K.; Taira, K. *J. Am. Chem. Soc.* **2004**, *126*, 744−752.
(9) (a) Smith, J. S.; Nikonowicz, E. P. *Biochemistry* **2000**, 39, 5642−5652. (b) Reiter, N. J.; Nikstad, L. J.; Allmann, A. M.; Johnson, R. J.; Butcher, S. E. *RNA* **2003**, 9, 533−542.

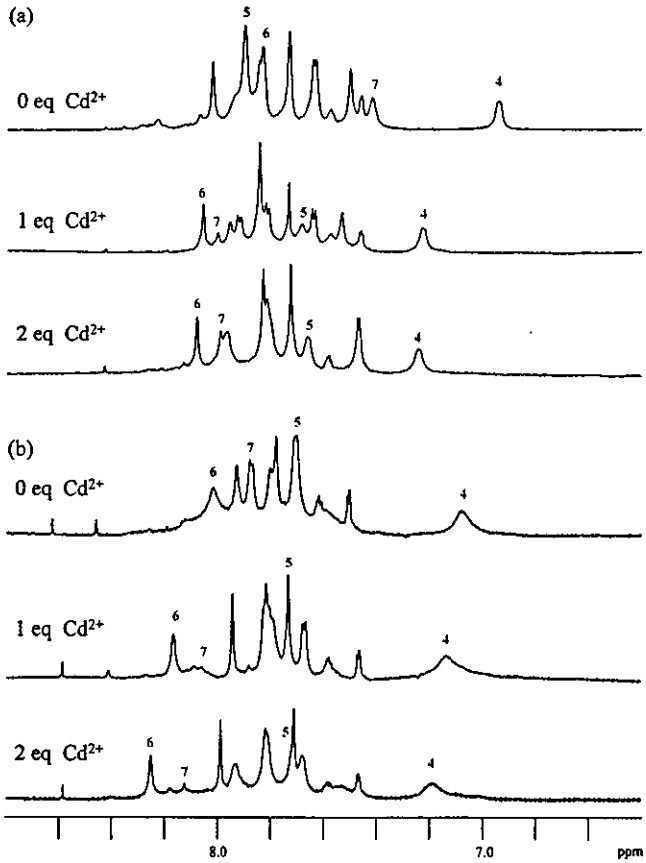

Figure 2. ^{1}H NMR spectra of GA10*Sp*S (a) and GA10*Rp*S (b). The spectra were recorded from samples dissolved in a solution of 40 mM $NaClO_4$ in 10 mM sodium cacodylate buffer at pH 7.6 in a 3-mm NMR tube at 40 °C. The concentrations, as duplexes, of GA10*Sp*S and GA10*Rp*S were 1.77 mM and 1.62 mM, respectively. From the top to the bottom in (a) and (b), the number of molar equivalents of $CdCl_2$ relative to the RNA was 0, 1, and 2, as indicated. Important signals of H8/H6 protons are labeled with respective residue numbers.

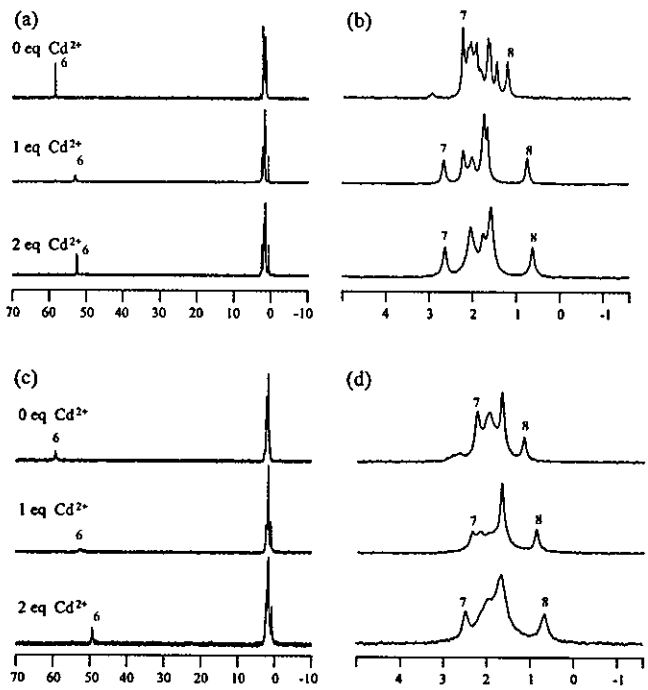

Figure 3. ^{31}P NMR spectra of GA10*Sp*S (a) and GA10*Rp*S (c). Expanded regions of the spectra are displayed in (b) and (d), respectively. The spectra were recorded from solutions of 40 mM $NaClO_4$ in 10 mM sodium cacodylate buffer at pH 7.6 in a 3-mm NMR tube at 40 °C. The concentrations, as a duplex, of GA10*Sp*S and GA10*Rp*S were 1.77 mM and 1.62 mM, respectively. From the top to the bottom in each group, the number of molar equivalents of $CdCl_2$ relative to the RNA was 0, 1, and 2, as indicated. With increasing concentrations of Cd^{2+} ions, signals from both the *Rp*- and the *Sp*-phosphorothioate (*Sp*, 58.5 ppm; and *Rp*, 59.7 ppm, in the absence of Cd^{2+} ions) shifted toward a higher field. Important signals are labeled with their respective residue numbers.

namely GA10.[8] GA10*Sp*S can capture metal ions in the same manner as GA10. By contrast, the ^{1}H chemical shifts of GA10*Rp*S around the P9 phosphorothioate moiety were different from those of the parental GA10 in the absence of Cd^{2+} ions, suggesting that the introduction of a bulky sulfur atom at the P9 site had adversely affected the conformation. However, the shift of signals from GA10*Rp*S that was induced by Cd^{2+} ions was similar to that observed with GA10. Thus, the addition of Cd^{2+} ions caused a change in and a correction of conformation of GA10*Rp*S and the resultant, induced and "corrected" metal-binding form was identical to that of GA10. These result suggests that the introduction of a sulfur atom at the pro-*Rp* position of A9/G10.1 can change the conformation of the ribozyme and that this conformational change has a negative effect on the hammerhead reaction, whereas the corresponding replacement at the pro-*Sp* position does not influence the structure of the hammerhead ribozyme and does not affect the catalytic activity. Since the structure of a ribozyme with an *Rp*-phosphorothioate in the absence of thiophilic metal ions is different from that of the natural ribozyme in the absence of those thiophilic metal ions, reactions catalyzed by these two different ribozymes in the presence of only hard metal ions can be quite different from each other.

While, it is still generally accepted, on the basis of the first crystal structure and kinetic studies, that coordination of a metal ion at the A9 pro-*Rp* oxygen at A9/G10.1 is essential for hammerhead catalysis, our present analysis argues against the previous interpretation. Our data and previous structural and kinetic data can best be interpreted if we simply assume that the introduction of a sulfur atom at the *Rp*-position but not at the *Sp*-position deforms the active conformation of the ribozyme and that a Cd^{2+} ion can interact with either an *Rp*- or an *Sp*-phosphorothioate at the A9/G10.1 site to generate an active ribozyme. The reduced rate of cleavage by the *Rp*-phosphorothioate appeared to be due to the negative effects of the structural change that were induced by the sulfur atom of the *Rp*-phosphorothioate. Thus, care must be taken in the interpretation of thio-effects and Cd^{2+}-rescue effects in kinetic analyses.[1h,10]

Results

One-Dimensional (1D) ^{1}H and ^{31}P NMR and Two-Dimensional (2D) Natural-Abundance ^{1}H-^{13}C HSQC Spectroscopy. It has been reported that changes in chemical shifts of bases and phosphate groups provide evidence of the binding of metal ions and conformational changes.[8b,c,11] In this study, we examined chemical shifts in ^{1}H, ^{31}P, and ^{13}C NMR spectra in an effort to elucidate the structural changes in GA10*Sp*S and GA10*Rp*S that occur upon the addition of Cd^{2+} ions. The 1D ^{1}H and ^{31}P NMR spectra are shown in Figure 2 and Figure 3, respectively. It was impossible to detect signals from base carbons directly because of the low concentrations of our samples. We used natural abundance ^{1}H-^{13}C HSQC spectra

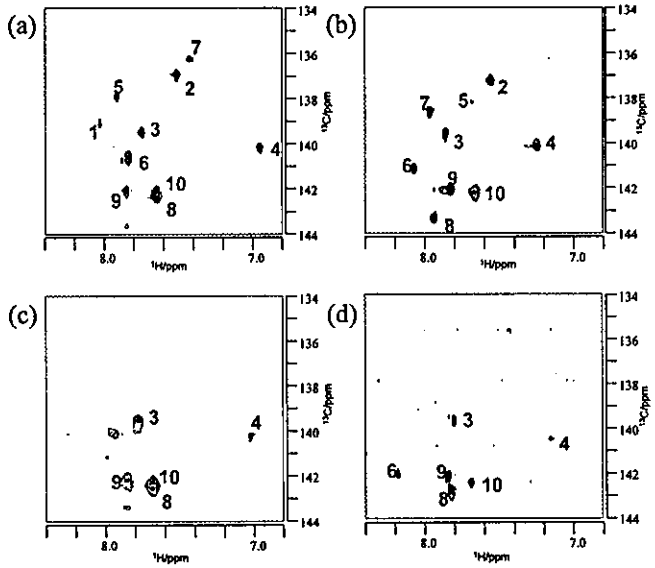

Figure 4. Natural-Abundance ^{1}H-^{13}C HSQC spectra of GA10*Sp*S in the absence of Cd^{2+} ions (a), of GA10*Sp*S in the presence of 1 molar equivalent of Cd^{2+} ions (b), of GA10*Rp*S in the absence of Cd^{2+} ions (c), and of GA10*Rp*S in the presence of 1 molar equivalent of Cd^{2+} ions (d). Intraresidue cross-peaks are labeled with their respective residue numbers.

for indirect detection of C6/C8 ^{13}C chemical shifts (Figure 1d and Figure 4).

The samples for NMR spectroscopy contained 1.77 mM GA10*Sp*S or 1.62 mM GA10*Rp*S as a duplex and 40 mM $NaClO_4$ at pH 7.6, plus $^{113}CdCl_2$, at various concentrations, namely, 0, 1.77 and 3.54 mM for GA10*Sp*S and 0, 1.62 and 3.24 mM for GA10*Rp*S. These concentrations of $CdCl_2$ corresponded to 0, 1 and 2 molar equivalents relative to GA10*Sp*S and GA10*Rp*S as a duplex. At each concentration of $CdCl_2$, we recorded the ^{1}H and ^{31}P NMR spectra and the ^{1}H-^{13}C HSQC spectra in D_2O at 40 °C.

Effects of the Sulfur Atom on the Structure of GA10*Sp*S and GA10*Rp*S in the Absence of Cd^{2+} ions. The signals due to the H6 and H8 protons of GA10*Sp*S and GA10*Rp*S in Figure 2 were assigned by reference to NOESY spectra. The H8 protons of G7 and G5 differed significantly between GA10*Sp*S and GA10*Rp*S. The chemical shift of the H8 proton of G7 (7.88 ppm) in GA10*Rp*S was significantly lower-field than that of GA10*Sp*S (7.42 ppm), suggesting a difference in conformation. The profile of the ^{31}P signals from GA10*Rp*S were broader than those from GA10*Sp*S. However, the ^{31}P chemical shifts for GA10*Sp*S and GA10*Rp*S were almost the same, as shown in Figure 3. Table 1 shows the assignments of ^{1}H and ^{31}P NMR signals in the absence of Cd^{2+} ions and the differences in chemical shifts relative to most of the parental GA10, which does not include a phosphorothioate moiety. The signals due to the protons of GA10*Sp*S were almost identical to those of GA10. The chemical shifts are different only by ±0.02 ppm.

The signals due to the protons of GA10*Rp*S were not the same as those of GA10. In particular, signals associated with C4, G5, A6, and G7 were very different from those of GA10. These results indicate that the effect of the sulfur atom on the structure of GA10*Sp*S was negligible but the effect of the sulfur atom on the structure of GA10*Rp*S was large, probably because the *R*p-sulfur atom is located toward the inside in the major groove that is a crowded position. The inserted sulfur atom in GA10*Rp*S apparently changed the structure from that of the

Table 1. ^{1}H (H6/H8) and ^{31}P Chemical Shifts (ppm) of GA10*Sp*S and GA10*Rp*S at 40 °C in the Absence of Cd^{2+} Ions and Differences in Chemical Shifts from Those of GA10

	GA10*Sp*S				GA10*Rp*S			
	^{1}H (H6/H8)		^{31}P		^{1}H (H6/H8)		^{31}P	
base no.	ppm[a]	Δ[c]	ppm[b]	Δ[c]	ppm[a]	Δ[d]	ppm[b]	Δ[d]
1	8.02	0.01			8.02	0.01		
2	7.50	0.02	2.12	−0.08	7.62	0.14	2.23	0.03
3	7.73	−0.02	1.93	0	7.80	0.05	1.95[e]	0.02
4	6.94	−0.02	2.06	−0.03	7.07	0.11	1.95[e]	−0.14
5	7.90	0.01	1.46	−0.15	7.70	−0.19	1.66	0.05
6	7.83	−0.01	58.5	56.15	8.02	0.18	59.37	57.02
7	7.42	0	2.24	−0.03	7.88	0.46	2.23	−0.04
8	7.64	−0.02	1.22	0.06	7.70	0.04	1.16	0
9	7.85	0	1.66	−0.04	7.88	0.03	1.66[e]	−0.04
10	7.64	−0.01	1.62	−0.04	7.70	0.05	1.66[e]	0

[a] Relative to DSS. [b] Relative to 85% H_3PO_4. [c] The difference in chemical shifts (GA10*Sp*S−GA10). [d] The difference in chemical shifts (GA10*Rp*S−GA10). [e] Tentative assignment since the signal was broadening and no correlation could be obtained in the ^{1}H−^{31}P HMQC NOESY spectrum.

parental GA10. Although the only difference between GA10*Rp*S and GA10 is the replacement of an oxygen atom by a sulfur atom in the former at the pro-*Rp* position of A6, the conformation of GA10*Rp*S was not identical to that of GA10. Although the H8 proton of G2 in GA10*Rp*S is away from the metal binding site, the thiolation affected the chemical shift of this proton more than that of C4 though the origin of this shift is unknown (Table 1). However, the chemical shifts of ^{31}P signals were almost the same for GA10*Rp*S and GA10, suggesting that the conformation of the backbone of GA10*Rp*S was almost identical to that of GA10.[12] Thus, the effect of the sulfur atom in GA10*Rp*S appeared to be local and limited to the region around the A6 position, which is considered to be the metal-binding site.

The ^{1}H-^{13}C HSQC spectrum (Figure 4) in the absence of Cd^{2+} ions was consistent with the results deduced from the 1D ^{1}H and ^{31}P spectra. The ^{1}H-^{13}C HSQC spectrum of GA10*Sp*S (Figure 4a) was almost identical to that of GA10,[8d] whereas the spectrum of GA10*Rp*S (Figure 4c) differed from that of GA10. The cross-peaks associated with G5, A6, and G7 were missing from the HSQC spectrum of GA10*Rp*S, suggesting that this metal-binding region around A6 might be associated with midrange chemical exchange on the NMR time-scale and might adopt multiple conformations locally. From the 1D ^{1}H and ^{31}P NMR spectra and the natural-abundance ^{1}H-^{13}C HSQC spectra, we deduced that the structure of GA10*Sp*S was almost identical to that of the parental and unmodified metal-binding motif, GA10, whereas the structure of GA10*Rp*S differed locally from the structure of GA10 around the metal-binding site in the absence of thiophilic Cd^{2+} ions. Furthermore, it appeared that midrange chemical exchange occurred around the metal-binding site of GA10*Rp*S.

(10) (a) Zhou, D. M.; Kumar, P. K. R.; Zhang L. H.; Taira K. *J. Am. Chem. Soc.* **1996**, *118*, 8969−8970. (b) Zhou, D. M.; Taira K. *Chem. Rev.* **1998**, *98*, 991−1026.
(11) (a) Wilson, W. D.; Heyl, B. L.; Reddy, R.; Marzilli, L. G. *Inorg. Chem.* **1982**, *21*, 2527−2528. (b) Pecoraro, V. L.; Hermes, J. D.; Cleland, W. W. *Biochemistry* **1984**, *23*, 5262−5271. (c) Jia, X.; Zon, G.; Marzilli, L. G. *Inorg. Chem.* **1991**, *30*, 228−239. (d) Mukundan, S., Jr.; Xu, Y.; Zon, G.; Marzilli, L. G. *J. Am. Chem. Soc.* **1991**, *113*, 3021−3027. (e) Legault, P.; Hoogstraten, C. G.; Metlitzky, E.; Pardi, A. *J. Mol. Biol.* **1998**, *284*, 325−335.
(12) Fürtig, B.; Richter, C.; Wöhnert, J.; Schwalbe, H. *ChemBioChem* **2003**, *4*, 936−962.

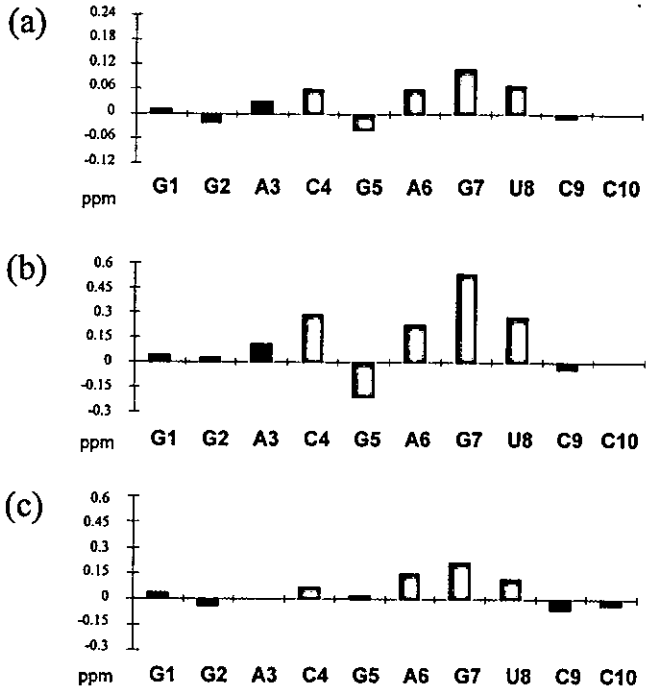

Figure 5. Changes in ^{1}H chemical shifts of H6/H8 protons of GA10 (a), GA10*Sp*S (b) and GA10*Rp*S (c) upon the addition of 1 molar equiv of Cd^{2+} ions.

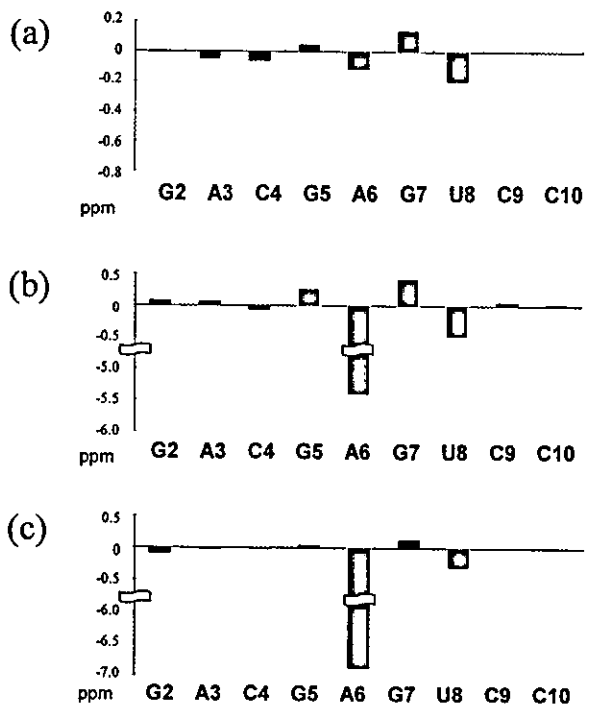

Figure 6. Changes in ^{31}P chemical shifts of phosphate signals of GA10 (a), GA10*Sp*S (b) and GA10*Rp*S (c) with the addition of one molar equiv of Cd^{2+} ions.

Perturbations Caused by Cd^{2+} Ions in GA10*Sp*S and GA10*Rp*S. The ^{1}H signals of GA10*Sp*S and GA10*Rp*S shifted upon the addition of Cd^{2+} ions (Figure 2). The changes of the chemical shifts are summarized in Figure 5 in a comparison with those for GA10. It should be noted that this decamer is self-complementary, thus, it contains two possible metal binding sites, and the addition of 1 molar equivalent Cd^{2+} will only occupy one site. However, because of the symmetry and fast-exchange, the observed ^{1}H NMR spectra for GA10*Sp*S and GA10*Rp*S were averaged singly metal-occupied structure. The changes in chemical shifts for GA10*Sp*S upon the addition of Cd^{2+} ions were similar to those for GA10. The proton signals associated with C4, A6, G7, and U8 moved largely downfield and the proton signal associated with G5 moved upfield upon the addition of Cd^{2+} ions to GA10*Sp*S (Figure 5b). These changes were almost identical to those of GA10 (Figure 5a). The signals for GA10*Sp*S were almost identical to those of GA10 not only in the absence of Cd^{2+} ions but also in the presence of Cd^{2+}, suggesting that these two motifs had similar conformations despite the introduction of a bulky sulfur atom at the *Sp*-position of the P9 phosphate in GA10*Sp*S.

Although the movements of signals were not as large as those of signals from GA10*Sp*S, the actual number of shifted signals from GA10*Rp*S was similar to the number from GA10 (Figure 5c), suggesting that metal coordination occurred around the same region of GA10. Moreover, the proton signals associated with C4, A6, G7, and U8 also moved downfield. Thus, we can conclude, from the movement of ^{1}H signals, that the final form of GA10*Rp*S with bound metal ions was similar to that of GA10 with bound metal ions. In other words, although the conformation of GA10*Rp*S in the absence of Cd^{2+} ions was different from that of GA10, the added Cd^{2+} ions were able to induce a conformational change in GA10*Rp*S such that it adopted a conformation similar to that of GA10 with bound Cd^{2+} ions. Note that the vertical scales for GA10*Sp*S and GA10*Rp*S in Figure 5 are different from that for GA10. The changes in chemical shifts of GA10*Sp*S and GA10*Rp*S in ^{1}H NMR spectra were larger than those of GA10. The larger size of the changes in chemical shifts of GA10*Sp*S and GA10*Rp*S that were induced by the sulfur atom and Cd^{2+} ions can be explained by the *H*ard and *S*oft *A*cid *B*ase (HSAB) rule.[13] Thus, a 'soft acid', such as a Cd^{2+} ion, prefers to bind to a sulfur atom, which is a 'soft base' (within GA10*Sp*S and GA10*Rp*S) than to an oxygen atom, which is a 'hard base' (within GA10).

Figure 6 shows the changes in ^{31}P chemical shifts of signals from GA10*Sp*S and GA10*Rp*S upon the addition of Cd^{2+} ions, in a comparison with GA10. The changes in signals for GA10*Sp*S (Figure 6b) and GA10*Rp*S (Figure 6c) were similar to those for GA10 (Figure 6a). Since the sulfur atom of the phosphorothioate moiety binds more tightly to a Cd^{2+} ion than does an oxygen atom, the signals associated with A6 within GA10*Sp*S and GA10*Rp*S moved largely upfield. The shifts in the ^{31}P signal of the phosphorothioate were 5.4 and 6.87 ppm for GA10*Sp*S and GA10*Rp*S, respectively, upon the addition of 1 molar equiv of Cd^{2+} ions. The ^{31}P signals associated with G5 and G7 moved downfield and those of U8 moved upfield in all these oligomers. The directions of the movements of these respective signals from GA10*Sp*S and GA10*Rp*S were identical to those from GA10, indicating that the structures of GA10*Sp*S and GA10*Rp*S were changed by binding of Cd^{2+} ions and that the metal-bound forms of GA10*Sp*S and GA10*Rp*S were similar to that of GA10.[12]

The changes in ^{13}C chemical shifts for GA10*Sp*S also resembled those for GA10 (Figure 4).[8b] The cross-peaks associated with G5, A6, G7, and U8 moved considerably and the directions of movements of respective cross-peaks were identical to those for GA10 (Figure 4, parts a and b). In the

(13) (a) Pearson, R. G. *J. Chem. Educ.* **1968**, *45*, 581–587. (b) Pearson, R. G. *J. Chem. Educ.* **1968**, *45*, 643–648.

case of GA10*Rp*S, although cross-peaks associated with G5 and G7 were not detected, the cross-peak associated with A6 emerged upon the addition of Cd^{2+} ions (Figure 4, parts c and d). The cross-peak associated with U8 in GA10*Rp*S shifted in the same direction as that in GA10. It appeared, from our analysis of the movements of ^{1}H, ^{31}P and ^{13}C resonances, that the structural changes in GA10*Sp*S and GA10*Rp*S that accompany coordination of a thiophilic metal ion resemble to those in GA10 and lead, eventually, to the similar active form upon the addition of appropriate metal ions.

Discussion

In this report, we described the characterization of the metal-binding forms of GA10*Sp*S and GA10*Rp*S, which correspond to the metal-binding motif of the A9/G10.1 site in a hammerhead ribozyme, by monitoring ^{1}H, ^{31}P, and ^{13}C NMR signals. GA10*Sp*S and GA10*Rp*S contained a phosphorothioate moiety at A6, which correspond to A9 in a hammerhead ribozyme and appear to be a metal-binding site. The ^{1}H and ^{13}C resonances of H6/H8 and C6/C8 atoms provided information about local structural changes around the A6 metal-binding sites of GA10*Sp*S and GA10*Rp*S. Comparisons of changes in chemical shifts with and without a sulfur atom at the A9/G10.1 site revealed the positional effect of the sulfur atom at P9 and the role of the pro-*Sp* oxygen and the pro-*Rp* oxygen at the A9/G10.1 site of hammerhead ribozymes.

Conformation of GA10*Sp*S and GA10*Rp*S in the Absence of Cd^{2+} Ions: The Effects of a Sulfur Atom at the pro-*Rp* and pro-*Sp* Positions on Structure. The effects of a sulfur atom on structure differed between GA10*Sp*S and GA10*Rp*S. The chemical shifts of the ^{1}H, ^{13}C, and ^{31}P signals of GA10*Sp*S were almost identical to those of GA10 (Figure 2a, 3a, 4a, and Table 1). These results imply that the tertiary structures of GA10*Sp*S and GA10 are similar and that the sulfur atom in GA10*Sp*S does not induce a structural change. By contrast to those of GA10*Sp*S, the ^{1}H and ^{13}C signals of GA10*Rp*S were different from those of GA10 in the absence of Cd^{2+} ions (Figure 2b, 4c, and Table 1). Although the line shape of ^{31}P signals from GA10*Rp*S was broadened (Figure 3, parts c and d), the chemical shifts were similar to those of signals from GA10 except at position 6, which corresponded to the phosphorothioate linkage (Table 1). Therefore, the results indicate that the sulfur atom of GA10*Rp*S induced a conformational change around the metal-binding site of A6 but the backbone structure of GA10*Rp*S was unaffected.[12] The radius of a sulfur atom is 1.85 Å and is 0.45 Å larger than that of an oxygen atom. The length of a P−S bond is 1.8 Å and is 0.3 Å longer than that of a P−O bond. Moreover, the pro-*Rp* oxygen is located toward the inside in the major groove in the crystal structure and this location might not allow for any steric hindrance in the ribozyme's structure. The larger-radius sulfur atom, the longer P−S bond and the resultant steric hindrance by the pro-*Rp* sulfur are likely to have induced a conformational change around the P9 metal-binding site and to have had a negative effect on the conformation of the ribozyme.

Binding of Metal Ions to GA10*Sp*S and GA10*Rp*S. In the previous study using a full-length hammerhead ribozyme, ^{31}P NMR signals of both *Rp*- and *Sp*-phosphorothioates shifted 2-3 ppm upfield upon the addition of 1 to 2 molar equiv of Cd^{2+} ions.[6] Similar changes were observed for the metal-binding motifs consisting solely of short GA10*Sp*S and GA10*Rp*S, although the magnitude of the upfield shift (5-7 ppm) upon addition of 1 equiv of Cd^{2+} was greater for the short oligomers probably because the full-length ribozyme might have more nonspecific interactions and/or specific interactions at site(s) other than the A9/G10.1 site between phosphates and Cd^{2+} ion-(s) that had increased the end-point by Cd^{2+} saturation. Nevertheless, since a Cd^{2+} ion can interact with *Rp*- and *Sp*-phosphorothioates in the metal-binding motif of both the full-length ribozyme and the shortened GA10*Sp*S and GA10*Rp*S and since complete assignments of ^{1}H, ^{13}C and ^{31}P signals were possible only for the short oligos, we in this study used GA10*Sp*S and GA10*Rp*S. Indeed, perturbations occurred not only in the ^{31}P signal from the inserted phosphorothioate (A6) but also in most of the ^{1}H, ^{13}C and ^{31}P signals, suggesting that there might have been a conformational change in both GA10*Sp*S and GA10*Rp*S as a result of the binding of Cd^{2+} ions. The perturbations in signals from GA10*Sp*S were almost identical to those from GA10. Thus, the Cd^{2+}-binding form in GA10*Sp*S was similar to that of GA10. In GA10*Rp*S, even though the chemical shifts in the ^{1}H NMR spectrum in the absence of metal ions, in particular at the H6 and H8 positions, were different from those in GA10, the perturbations induced by Cd^{2+} ions resembled the perturbations induced by Cd^{2+} ions in GA10 (Figures 5 and 6). It is noteworthy that the conformation not only of GA10*Sp*S with a bound metal ion but also of GA10*Rp*S with a bound metal ion was similar to that of GA10 with a bound metal ion, even though, in the absence of metal ions, the conformation of GA10*Rp*S was different from that of GA10.

Does a metal ion bind directly or indirectly to N7 and the phosphate oxygen at the A9/G10.1 metal-binding site? In a previous study, using ^{15}N-labeled GA10, we did not detect any coupling between the N7 atom at G7 and $^{113}Cd^{2+}$, even though signal perturbation occurred at this N7 atom and the C8 atom of G7.[8c] The binding of metal ions by GA10*Sp*S and GA10*Rp*S was stronger than that by GA10 because the phosphorothioate moiety contained a sulfur atom at the metal-binding site. The HSAB rule determines that a 'hard acid', such as a Mg^{2+} ion, prefers to bind to an oxygen atom. Before the titration of the phosphorothioate with Cd^{2+} ions, we expected that coupling might be evident, in the ^{31}P signal of A6 and the H8/C8 cross-peak of G7 in the ^{1}H-^{13}C HSQC spectra of GA10*Rp*S and GA10*Sp*S in the presence of one molar equivalent of Cd^{2+} ions, assuming that binding of metal ions would involve direct coordination.[14] No coupling between ^{31}P of A6 and ^{113}Cd (Figure 3, parts a and c) or between the H8 atom of G7 and ^{113}Cd (Figure 2, parts a and b) was detected in this study, even though large perturbations in chemical shifts were noted in the ^{31}P and ^{1}H NMR spectra.

Theoretical calculations of spin coupling constants and chemical shifts related to the binding of a divalent metal ion to guanine were reported recently.[15] The calculated chemical shift of the N7 atom of guanine for an inner-shell binding complex of Mg^{2+} ion with guanine is similar to the chemical shift detected experimentally by our group.[8d] The theoretical calcula-

(14) Damblon, C.; Prosperi, C.; Lian, L.-Y.; Barsukov, I.; Soto, R. P.; Galleni, M.; Frere, J.-M.; Roberts, G. C. K. *J. Am. Chem. Soc.* **1999**, *121*, 11575−11576.

(15) Sychrovsky, V.; Sponer, J.; Hobza, P. *J. Am. Chem. Soc.* **2004**, *126*, 663−672.

tions supported the direct coordination of a metal ion to the N7 atom of guanine,[15] suggesting the same conclusion as the one that we had reached on the basis of our experiments.[8d] The theoretical calculations, indicated that the change in chemical shift of the signal due to the C8 atom of G7 in the ^{1}H-^{13}C HSQC spectrum of GA10*Sp*S (Figure 4, parts a and b) implies the direct coordination of a Cd^{2+} ion to the N7 atom of G7,[15] although outer-sphere coordination cannot completely be ignored.[16] The coupling was absent in the present study, in which we used a sulfur atom and ^{113}Cd ions, because of rapid exchange of Cd^{2+} ions at the metal-binding site, although we cannot completely exclude the possibility of coupling between $^{113}Cd^{2+}$ and H8 of G7 in the case of the full length hammerhead ribozyme.

Pro-*Rp* Phosphorothioate at A9 of a Hammerhead Ribozyme. Kinetic studies of constructs with a phosphorothioate moiety at the A9/G10.1 site of hammerhead ribozymes suggested the important metal-binding role of the pro-***Rp*** oxygen but not of the pro-***Sp*** oxygen since the pro-***Rp*** sulfur-substituted ribozyme was inactive in Mg^{2+}-mediated reactions but was rescued by the addition of thiophilic Cd^{2+} ions. The corresponding pro-***Sp*** sulfur-substituted ribozyme was active even in Mg^{2+}-mediated reactions. However, this interpretation requires the assumption that the sulfur atom of the phosphorothioate does not affect the initial conformation of the hammerhead ribozyme, nor the corresponding structures in the presence of hard Mg^{2+} ions. If the inserted sulfur atom were to influence the conformation of the hammerhead ribozyme, then we would have to consider the effects of this conformation change in our interpretation of the kinetic results obtained with the phosphorothioate. In other words, the conformational change caused by insertion of sulfur might disrupt the ribozyme reaction if the conformation of the phosphorothioate-containing ribozyme is not an active conformation.

We demonstrated in the present study that, in the absence of metal ions, a conformational change does indeed occur as a result of the sulfur in GA10***Rp***S but it does not occur in GA10***Sp***S. Therefore, we can postulate that the conformation of the hammerhead ribozyme that contains a phosphorothioate moiety at the pro-***Rp*** of A9 is likely to be different from that of the wild-type ribozyme, whereas the hammerhead ribozyme that contains a phosphorothioate moiety at the pro-***Sp*** of A9 retains the conformation of the wild-type ribozyme. The decreased rate of the reaction catalyzed by the ribozyme that contains a phosphorothioate moiety at the pro-***Rp*** site means that the conformational change induced by the phosphorothioate has a negative effect on the ribozyme reaction. It appears that the rescue by Cd^{2+} ions in kinetic studies is due to the recovery of an active metal-associated form that resembles the metal-associated form of the wild-type ribozyme (remember that the changes in chemical shifts induced by Cd^{2+} ions in GA10***Rp***S were similar to those induced by Cd^{2+} ions in GA10).

In summary, we examined conformational changes upon the interaction of Cd^{2+} ions with the A9/G10.1 metal-binding motif of a hammerhead ribozyme. Our analysis demonstrated that the effects of the introduction of a phosphorothioate linkage at a specific position depend on whether the sulfur is at the pro-***Rp*** or the pro-***Sp*** position. Since the effects at the two positions are not the same, the resultant conformers are likely to be at different energy levels or, in catalytic nucleic acids, they are likely to have different activities, a possibility that has been ignored in the past. Indeed, two observations can be most simply and best explained by this conclusion. The first of these two observations is that the pro-***Rp*** sulfur-substituted ribozyme is inactive in Mg^{2+}-mediated reactions but its activity can be rescued by the addition of thiophilic Cd^{2+} ions, whereas the corresponding pro-***Sp*** sulfur-substituted ribozyme is active even in Mg^{2+}-mediated reactions. The second observation is that the conformation of GA10***Sp***S is similar to that of the parental GA10, whereas the conformation of GA10***Rp***S is different from that of the parental GA10 in the absence of Cd^{2+} ions, even though all oligomers yield similar Cd^{2+}-bound forms. Thus, the introduction of sulfur at the pro-***Rp*** position but not at the pro-***Sp*** position disturbs the active conformation of the ribozyme. Our analysis clearly warns against incautious interpretations of thio-effects and rescue phenomena because the previous assumption that the two different conformers have the same effects, other than the effects of position, is clearly not always valid.

Experimental Section

Preparation of Samples. A crude mixture of the GA10***Rp***S and GA10***Sp***S phosphorothioate isomers was purchased from Genset Corporation (France). The two components of the mixture were separated and purified as described previously.[7] Assignments of isomers were made after digestion by snake venom phosphodiesterase and nuclease P1.[17] For digestion by snake venom phosphodiesterase, an aliquot of each thio-substituted oligonucleotide (0.5 nmol) was incubated for 8 h at 37 °C with snake venom phosphodiesterase (0.1 μg; Sigma-Aldrich, USA) and calf alkaline phosphatase (6.0 μg; Takara, Japan) in 0.05 M Tris-HCl (pH 9.0), 0.3 mM DTT and 1 mM $MgCl_2$ in a total volume of 150 μL. The products were analyzed directly by HPLC on a reversed-phase column (TSK-GEL ODS-80TM; length, 250 mm; i.d., 4.6 mm; Tosoh, Japan) with a gradient of buffer A, namely, 0.1 M triethylammonium acetate (pH 7.0), and buffer B, which consisted of 60% buffer A and 40% acetonitrile (5% B for 15 min followed by 5% to 100% B over the course of 45 min). Retention times under these conditions were as follows: cytidine, 2.86 min; uridine, 5.89 min; guanosine, 8.02 min; and adenosine, 12.31 min. The products of digestion of the later-eluting isomer generated a peak at 25.87 min that corresponded to *Sp*-GpsA. For digestion by nuclease P1, an aliquot of each thio-substituted oligonucleotide (0.5 nmol) was digested with nuclease P1 (2.0 μg; Sigma-Aldrich) in distilled water (120 μL) for 1 h at 37 °C. The solution was buffered with 16 μL of 50 mM Tris-HCl (pH 9.0) and digested with calf alkaline phosphatase (6.0 μg; Takara) for 1 h at 37 °C. The products were analyzed by reversed-phase HPLC as described above. The products of digestion of the earlier-eluting isomer generated a peak at 24.46 min that corresponded to *Rp*-GpsA.

Resonance Assignments. Samples for NMR spectroscopy were prepared by dissolving purified oligomers in 60 μL of a

(16) Wang, G.; Gaffney, B. L.; Jones, R. A. *J. Am. Chem. Soc.* **2004**, *126*, 8908–8909.

(17) (a) Burgers, P. M.; Eckstein, F. *Biochemistry* **1979**, *18*, 592–596. (b) Almer, H.; Stawinski, J.; Strömberg, R. *J. Chem. Soc., Chem. Commun.* 1994, 1459–1460. (c) Stec, W. J.; Zon, G.; Egan, W.; Stec, B. *J. Am. Chem. Soc.* **1984**, *106*, 6077–6079. (d) Connolly, B. A.; Potter, B. V. L.; Eckstein, F.; Pingoud, A.; Grotjahn, L. *Biochemistry* **1984**, *23*, 3443–3453.

solution, prepared in D_2O, of 40 mM $NaClO_4$ and 10 mM sodium cacodylate buffer at pH 7.6 in a 3-mm NMR tube (Shigemi, Japan). The concentrations of GA10*Sp*S and GA10*Rp*S, each as a duplex were 1.77 mM and 1.62 mM, respectively. Concentrated solutions of $CdCl_2$ were added directly to each sample to give desired concentration. All NMR spectra were acquired on an INOVA 600 MHz NMR spectrometer (Varian, USA) operated at 40 °C, with a *z*-axis pulsed-field gradient probe. The chemical shifts of protons were determined relative to the signal from the internal standard, sodium 4,4-dimethyl-4-silapentane-1-sulfonate (DSS). The ^{31}P chemical shifts were referenced to an external 85% solution of H_3PO_4. Aromatic ^1H and ^{13}C resonances were assigned from ^1H-^1H NOESY, natural-abundance ^1H-^{13}C HSQC and ^1H-^{31}P HMQC NOESY spectra. Typical ^1H-^1H NOESY spectra were recorded with 4096 × 1024 complex points for a spectral width of 5071.0 Hz; 64 scans were averaged; and the mixing time was 300 ms. Natural-abundance ^1H-^{13}C HSQC spectra were recorded with 2048 × 160 complex points for a spectral width of 4743.8 × 6034.1 Hz, and 1408 scans were averaged. 2D ^1H-^{31}P HMQC NOESY spectra were recorded with 2048 × 32 complex points for a spectral width of 4821.6 × 1457.1 Hz; 2048 scans were averaged; and the mixing time for NOESY was 300 ms.

Acknowledgment. The authors thank Dr. Tanaka at Tohoku University and Dr. Furihata at Tokyo University for their helpful comments.

JA0472937

J|A|C|S
ARTICLES
Published on Web 09/11/2004

Analysis on a Cooperative Pathway Involving Multiple Cations in Hammerhead Reactions

Yasuomi Takagi,[†,‡] Atsushi Inoue,[†,§] and Kazunari Taira*[,†,§]

Contribution from the Gene Function Research Center, National Institute of Advanced Industrial Science and Technology (AIST), Central 4, 1-1-1 Higashi, Tsukuba Science City, 305-8562, Japan, iGENE Therapeutics, Inc., c/o AIST, Central 4, 1-1-1 Higashi, Tsukuba Science City, 305-8562, Japan, and Department of Chemistry and Biotechnology, School of Engineering, The University of Tokyo, Hongo, Tokyo 113-8656, Japan

Received December 29, 2003; E-mail: taira@chembio.t.u-tokyo.ac.jp

Abstract: The hammerhead ribozyme reaction is more complex than might have been expected, perhaps because of the flexibility of RNA, which would have enhanced the potential of RNA during evolution of and in the RNA world. Divalent Mg^{2+} ions can increase the rate of the ribozyme-catalyzed reaction by approximately 10^9-fold as compared to the background rate under standard conditions. However, the role of Mg^{2+} ions is controversial since the reaction can proceed in the presence of high concentrations of monovalent ions, such as Li^+, Na^+, and NH_4^+ ions, in the absence of divalent ions. We thus carried out ribozyme reactions under various conditions, and we obtained parameters that explain the experimental data. On the basis of the analysis, we propose a new pathway in the hammerhead ribozyme reaction in which divalent metal ions and monovalent ions act cooperatively.

Introduction

Catalytic RNAs that are found in nature include hammerhead, hairpin, hepatitis delta virus (HDV), and Varkud satellite (VS) ribozymes; Group I and II introns; and the RNA subunit of RNase P.[1-13] Furthermore, structural and chemical analyses strongly suggest that ribosomal RNA is a ribozyme,[14-18] and the possibility exists that the RNA component of the spliceosome might also be a ribozyme.[19] Early research on ribozymes suggested that all ribozymes might be metalloenzymes that require divalent metal ions, in particular Mg^{2+} ions, for catalysis, and that all might operate by a basically similar mechanism. However, extensive subsequent studies revealed that the catalytic activity of hairpin ribozymes is independent of divalent metal ions.[20-26] Although Group I and II introns and the RNA subunit of RNase P apparently exploit several divalent metal ions as catalysts,[27-34] the HDV ribozyme uses a combination of a divalent metal ion and a nucleobase,[35] while hairpin ribozymes seem to use a nucleobase only.[26] It has been suggested that ribosomal RNA also makes use of a nucleobase in the peptidyl transferase reaction rather than a divalent metal ion.[15-17] Thus, the various types of ribozyme appear to exploit different cleavage mechanisms, which depend, in turn, upon the architecture of each individual ribozyme.[36] Even hammerhead

† Gene Function Research Center, AIST.
‡ iGENE Therapeutics, Inc.
§ The University of Tokyo.

(1) Cech, T. R.; Zaug, A. J.; Grabowski, P. J. *Cell* **1981**, *27*, 487−496.
(2) Guerrier-Takada, C.; Gardiner, K.; Marsh, T.; Pace, N.; Altman, S. *Cell* **1983**, *35*, 849−857.
(3) Michel, F.; Umesono, K.; Ozeki, H. *Gene* **1989**, *82*, 5−30.
(4) Foster, A. C.; Symons, R. H. *Cell* **1987**, *50*, 9−16.
(5) Buzayan, J. M.; Gerlach, W. L.; Bruening, G. *Nature* **1986**, *323*, 349−353.
(6) Carola, C.; Eckstein, F. *Curr. Opin. Chem. Biol.* **1999**, *3*, 274−283.
(7) Hampel, A.; Tritz, R.; Hicks, M.; Cruz, P. *Nucleic Acids Res.* **1990**, *18*, 299−304.
(8) Feldstein, P. A.; Bruening, G. *Nucleic Acids Res.* **1993**, *21*, 1991−1998.
(9) Sharmeen, L.; Kuo, M. Y.-P.; Dinter-Gottlieb, G.; Taylor, J. *J. Virol.* **1988**, *62*, 2674−2679.
(10) Kuo, M. Y.-P.; Sharmeen, L.; Dinter-Gottlieb, G.; Taylor, J. *J. Virol.* **1988**, *62*, 4439−4444.
(11) Perrotta, A. T.; Been, M. D. *Nature* **1991**, *350*, 434−436.
(12) Lai, M. M. *Annu. Rev. Biochem.* **1995**, *64*, 259−286.
(13) Collins, R. A.; Seville, B. J. *Nature* **1990**, *345*, 177−179.
(14) Noller, H. F.; Hoffarth, V.; Zimniak, L. *Science* **1992**, *256*, 1416−1419.
(15) Nissen, P.; Hansen, J.; Ban, N.; Moore; P. B.; Steitz, T. A. *Science* **2000**, *289*, 920−930.
(16) Muth, G. W.; Ortoleva-Donnelly, L.; Strobel, S. A. *Science* **2000**, *289*, 947−950.
(17) Bayfield, M. A.; Dahlberg, A. E.; Schulmeister, U.; Dorner, S.; Barta, A. *Proc. Natl. Acad. Sci. U.S.A.* **2000**, *98*, 10096−10101.
(18) Cech, T. R. *Science* **2000**, *289*, 878−879.
(19) Collins, C. A.; Guthrie, C. *Nat. Struct. Biol.* **2000**, *10*, 850−854.
(20) Hampel, A.; Cowan, J. A. *Chem. Biol.* **1997**, *4*, 513−517.
(21) Nesbitt, S.; Hegg, L. A.; Fedor, M. J. *Chem. Biol.* **1997**, *4*, 619−630.
(22) Young, K. J.; Gill, F.; Grasby, J. A. *Nucleic Acids Res.* **1997**, *25*, 3760−3766.
(23) Chowrira, B. M.; Berzal-Herranz, A.; Burke, J. M. *Biochemistry* **1993**, *32*, 1088−1095.
(24) Earnshaw, D. J.; Gait, M. J. *Nucleic Acids Res.* **1998**, *26*, 5551−5561.
(25) Seyhan, A. A.; Burke, J. M. *RNA* **2000**, *6*, 189−198.
(26) Murray, J. B.; Seyhan, A. A.; Walter, N. G.; Burke, J. M.; Scott, W. G. *Chem. Biol.* **1998**, *5*, 587−595.
(27) Shan, S.; Yoshida, A.; Sun, S.; Piccirilli, J. A.; Herschlag, D. *Proc. Natl. Acad. Sci. U.S.A.* **1999**, *96*, 12299−12304.
(28) Yoshida, A.; Sun, S.; Piccirilli, J. A. *Nat. Struct. Biol.* **1999**, *6*, 318−321.
(29) Shan, S.; Kravchuk, A. V.; Piccirilli, J. A.; Herschlag, D. *Biochemistry* **2001**, *40*, 5161−5171.
(30) Gordon, P. M.; Sontheimer, E. J.; Piccirilli, J. A. *RNA* **2000**, *6*, 199−205.
(31) Gordon, P. M.; Sontheimer, E. J.; Piccirilli, J. A. *Biochemistry* **2000**, *39*, 12939−12952.
(32) Kurz, J. C.; Fierke, C. A. *Curr. Opin. Chem. Biol.* **2000**, *4*, 553−558.
(33) Warnecke, J. M.; Held, R.; Busch, S.; Hartmann, R. K. *J. Mol. Biol.* **1999**, *290*, 433−445.
(34) Pfeiffer, T.; Tekos, A.; Warnecke, J. M.; Drainas, D.; Engelke, D. R.; Seraphin, B.; Hartmann, R. K. *J. Mol. Biol.* **2000**, *298*, 559−565.
(35) Nakano, S.; Proctor, D. J.; Bevilacqua, P. C. *Biochemistry* **2001**, *40*, 12022−12038.
(36) Takagi, Y.; Warashina, M.; Stec, W. J.; Yoshinari, K.; Taira, K. *Nucleic Acids Res.* **2001**, *29*, 1815−1834.

10.1021/ja031991u CCC: $27.50